AD-A108 642 IOWA STATE UNIV AMES ENGINEERING RESEARCH INST F/G 13/11
PREDICTION OF LAMINAR-TO-TURBULENT BOUNDARY LAYER TRANSITION IN--ETC(U)
SEP 81 C E KLUCK AFOSR-81-0004
UNCLASSIFIED ISU-ERI-AMES-82030 AFOSR-TR-81-0806 NL

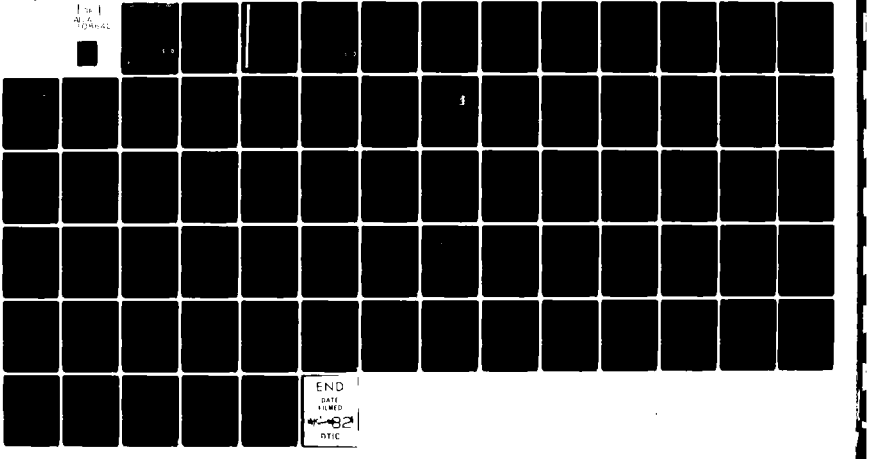

END
DATE FILMED
-82
DTIC

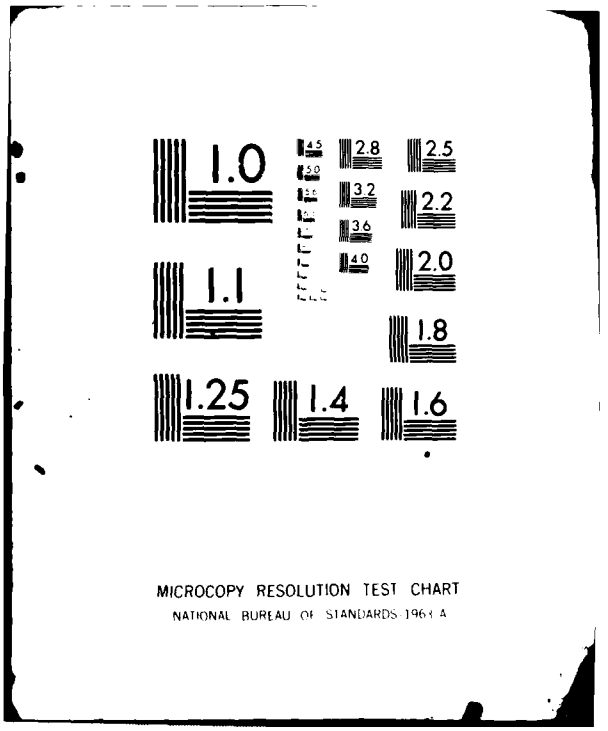
1.0
1.1
1.25
1.4
1.6
1.8
2.0
2.2
2.5
2.8
3.2
3.6
4.0
4.5
5.0
MICROCOPY RESOLUTION TEST CHART
NATIONAL BUREAU OF STANDARDS 1963 A

AFOSR-TR- 81-0806

LEVEL II

C. E. KLUCK
SEPTEMBER 1981

AD A108642

AFOSR- 81-0004

TECHNICAL REPORT

Prediction of Laminar-to-Turbulent Boundary Layer Transition in Axial-Flow Turbomachinery

DTIC
ELECTE
DEC 16 1981
S D

404418

Approved for public release;
distribution unlimited.

DTIC FILE COPY

TURBOMACHINERY
COMPONENTS RESEARCH PROGRAM

ISU-ERI-Ames-82030
TCRL-21
ERI Project-1491

ENGINEERING RESEARCH INSTITUTE
IOWA STATE UNIVERSITY
AMES, IOWA 50010 USA

81 12 14 062

UNCLASSIFIED
SECURITY CLASSIFICATION OF THIS PAGE (When Data Entered)

REPORT DOCUMENTATION PAGE		READ INSTRUCTIONS BEFORE COMPLETING FORM
1. REPORT NUMBER AFOSR-TR- 81-0806	2. GOVT ACCESSION NO. AD-A108642	3. RECIPIENT'S CATALOG NUMBER
4. TITLE (and Subtitle) PREDICTION OF LAMINAR-TO-TURBULENT BOUNDARY LAYER TRANSITION IN AXIAL-FLOW TURBOMACHINERY		5. TYPE OF REPORT & PERIOD COVERED INTERIM 1 OCT 80 - 30 SEP 81
		6. PERFORMING ORG. REPORT NUMBER
7. AUTHOR(s) CHARLES E KLUCK		8. CONTRACT OR GRANT NUMBER(s) AFOSR-81-0004
9. PERFORMING ORGANIZATION NAME AND ADDRESS IOWA STATE UNIVERSITY ENGINEERING RESEARCH INSTITUTE AMES, IA 50010		10. PROGRAM ELEMENT, PROJECT, TASK AREA & WORK UNIT NUMBERS 2307/A4 61102F
11. CONTROLLING OFFICE NAME AND ADDRESS AIR FORCE OFFICE OF SCIENTIFIC RESEARCH/NA BOLLING AIR FORCE BASE, DC 20332		12. REPORT DATE SEP 81
		13. NUMBER OF PAGES 67
14. MONITORING AGENCY NAME & ADDRESS(if different from Controlling Office)		15. SECURITY CLASS. (of this report) UNCLASSIFIED
		15a. DECLASSIFICATION/DOWNGRADING SCHEDULE

16. DISTRIBUTION STATEMENT (of this Report)

Approved for public release; distribution unlimited

17. DISTRIBUTION STATEMENT (of the abstract entered in Block 20, if different from Report)

18. SUPPLEMENTARY NOTES

19. KEY WORDS (Continue on reverse side if necessary and identify by block number)

AXIAL-FLOW COMPRESSOR
AXIAL-FLOW TURBINE
CASCADE AERODYNAMICS
BOUNDARY-LAYER TRANSITION

20. ABSTRACT (Continue on reverse side if necessary and identify by block number)

This paper first reviews current analytical studies regarding the laminar-to-turbulent boundary layer transition process, including relevant analysis of laminar separation, and then covers analytical and experimental studies concerning parametric effects on transition pertinent to axial-flow turbomachine blade rows. These include the effects of pressure gradient, freestream turbulence, surface roughness, heat transfer, and combined effects. Finally, the work of various authors who have established data correlations for transition on axial-

DD FORM 1 JAN 73 1473 EDITION OF 1 NOV 65 IS OBSOLETE

UNCLASSIFIED
SECURITY CLASSIFICATION OF THIS PAGE (When Data Entered)

flow turbomachine blade rows is evaluated. Their predictive equations and charts have been presented as a reference guide for determining the transition region on blades. Additionally, equations for calculating transitional boundary layer growth are presented.

ENGINEERING RESEARCH

ENGINEERING RESEARCH

ENGINEERING RESEARCH

ENGINEERING RESEARCH

ENGINEERING RESEARCH

TECHNICAL REPORT

Prediction of Laminar-to-Turbulent Boundary Layer Transition in Axial-Flow Turbomachinery

C. E. KLUCK

SEPTEMBER 1981

TURBOMACHINERY COMPONENTS RESEARCH LABORATORY
DEPARTMENT OF MECHANICAL ENGINEERING
ENGINEERING RESEARCH INSTITUTE
IOWA STATE UNIVERSITY, AMES

ISU-ERI-Ames-82030
TCRL-21
ERI Project-1491

TABLE OF CONTENTS

NOMENCLATURE

A_o	amplitude of initial disturbance
C_f	skin friction coefficient, $2\tau_w/\rho U^2$
C_L	aerodynamic lift coefficient, $L/\frac{1}{2}\rho U^2 x$ Area
c	compressor or turbine blade chord length
H	shape factor, δ^*/θ
i	blade incidence angle
k	surface roughness height
k_s	equivalent sand grain roughness size
l_1	length of laminar region in separation bubble up to transition, $x_t - x_s$
l_2	length of transition region in separation bubble up to the turbulent reattachment point, $x_T - x_t$
L	lift force
m_θ	pressure gradient parameter, $(\theta^2/\nu)\ dU/dx$
P_o	upstream stagnation pressure
Re_c	chord Reynolds number, $U_o c/\nu$
Re_{crit}	instability Reynolds number, Ux_i/ν
Re_δ	boundary layer thickness Reynolds number, $U\delta/\nu$
Re_{δ^*}	displacement thickness Reynolds number, $U\delta^*/\nu$
Re_θ	momentum thickness Reynolds number, $U\theta/\nu$
Tu	freestream turbulence intensity parameter, $\frac{\sqrt{u'^2}}{U}$
u	local x-direction boundary layer velocity
u'	local x-direction velocity fluctuation, rms
u_k	boundary layer velocity at top of roughness element
U	local freestream velocity

U_o incoming freestream velocity

U_s freestream velocity at the separation point

x general streamwise location

x_i streamwise location of instability point of neutral disturbances

x_s streamwise location of incipient laminar separation

x_t streamwise location of transition

x_T streamwise location of fully turbulent flow

Greek Symbols

δ boundary layer thickness

δ^* displacement thickness

γ intermittency factor for developing turbulence

λ Pohlhausen pressure gradient parameter, $(\delta^2/\nu)\ dU/dx$

θ momentum boundary layer thickness

θ_s momentum boundary layer thickness at the incipient laminar separation point

τ_w wall shear stress, $\mu(du/dy)_{y=0}$

ν kinematic fluid viscosity

ρ fluid density

μ absolute viscosity

1. INTRODUCTION

This paper summarizes a review of the literature on laminar-to-turbulent transition phenomena in incompressible flow. Emphasis has been placed on the transition process in subsonic axial-flow turbomachine blade rows, particularly compressor blade rows.

Accurately predicting transition in turbomachine blade rows is important. Increasing emphasis has been placed on modeling the loss characteristics of axial-flow compressors; these losses are correlated to the momentum thickness of the boundary layer at the trailing edge of the blades. Since the trailing edge boundary layer is often turbulent, the momentum thickness depends on location of the laminar-to-turbulent transition region. Also, the performance of compressors is adversely affected by the presence of laminar separation on the airfoil suction surface. Breakdown of the laminar boundary layer to turbulence prevents laminar separation and the accompanying performance deterioration. Prediction of the transition location, therefore, is an important requirement for compressor performance modeling.

Although the transition process has been studied for many years, the exact mechanism of transition is not fully understood. In fact, no successful analytical theory of boundary layer transition has been developed. Transition continues to elude theoretical prediction in terms of its initiation, duration, and forcing mechanism. On the macroscopic level, a number of different criteria are used to determine the onset of transition experimentally.

Two principal approaches are used to provide analytical transition

prediction. The first approach is linear stability theory, which predicts transition through the growth of unstable infinitesimal disturbances in the boundary layer. The second approach is turbulence modeling, which analyzes the developing presence of unstable waves through turbulent boundary layer equations.

This paper first reviews current analytical studies regarding the transition process, including relevant analysis of laminar separation, and then covers analytical and experimental studies concerning parametric effects on transition pertinent to axial-flow turbomachine blade rows. These include the effects of pressure gradient, freestream turbulence, surface roughness, heat transfer, and combined effects. Finally, the work of various authors who have established data correlations for transition on axial flow turbomachine blade rows is evaluated. Their predictive equations and charts have been presented as a reference guide for determining the transition region on blades. Additionally, equations for calculating transitional boundary layer growth are presented.

2. GENERAL TRANSITION MECHANISM

Laminar boundary layers formed on flat plates, curved surfaces, airfoils, or compressor cascades exhibit a strong tendency to break down into turbulence. Many factors, including surface roughness, freestream disturbances, and pressure gradient, contribute to this breakdown process. However, the principal cause of laminar-to-turbulent transition is the instability of laminar boundary layers to disturbances at sufficiently large Reynolds number.

According to White (1), transition is principally a development of the boundary layer from instability, where infinitesimal disturbances grow, to transition, where full-scale turbulence develops. However, White (1) states emphatically that no theory of transition exists, and that transition prediction relies on empirical and semi-empirical correlations of experimental data. Morkovin (2) reinforces this observation in his uncertainty principle for transition:

> "We shall never know enough about conditions and factors determining transition and a basic uncertainty will remain for accurate quantitative predictions."

2.1. Experimental Detection of Transition

A number of criteria are used in boundary layer studies to locate the transition region for airfoils experimentally. According to McDonald and Fish (3), transition begins at the point of minimum skin friction coefficient, C_f. Hall and Gibbings (4) use the minimum static pressure point as measured with a static pressure tap. Schlichting (5), however, suggests other criteria since the minimum pressure point is

near transition only at Re_c approximately 10^6. For larger values of Reynolds number, transition may occur upstream of minimum pressure (see Figure 1). Also, at smaller values of the lift coefficient C_L, locating the pressure minimum may become difficult because of "flatter" pressure distribution along the chord. Schlichting suggests that the sharp decrease in the shape factor H, as observed for flat plates, or a marked increase in the stagnation pressure may give a better indication.

A better indication is given by the intermittency factor γ. Intermittency factor is defined as the amount of time the boundary layer is turbulent during a given time span, with $\gamma = 1$ for fully turbulent flow. It is believed that the velocity distribution fluctuates between a laminar and turbulent profile during this time (5). Dunham (6) characterizes transition as that region where the intermittency increases from 0.25 to 0.75.

When measured by hot-wire anemometers, the transition region is characterized by a series of intermittent turbulent "bursts." These bursts take the form of high frequency velocity fluctuations in the range of 1 to 10^5 Hz, with a mean of about 1000 Hz. Amplitudes vary from 5 to 20% of the freestream velocity (7). These turbulent bursts, resulting from the coalescence of turbulent spots (8), are purely random in nature, covering the entire frequency spectrum without any indication of periodicity (1) (see Figure 2).

Other indicators of transition presented by Schlichting include an increase in the skin friction coefficient, an increase in the dynamic pressure measured at a constant boundary layer vertical location, and development of the fully developed turbulent flow velocity profile.

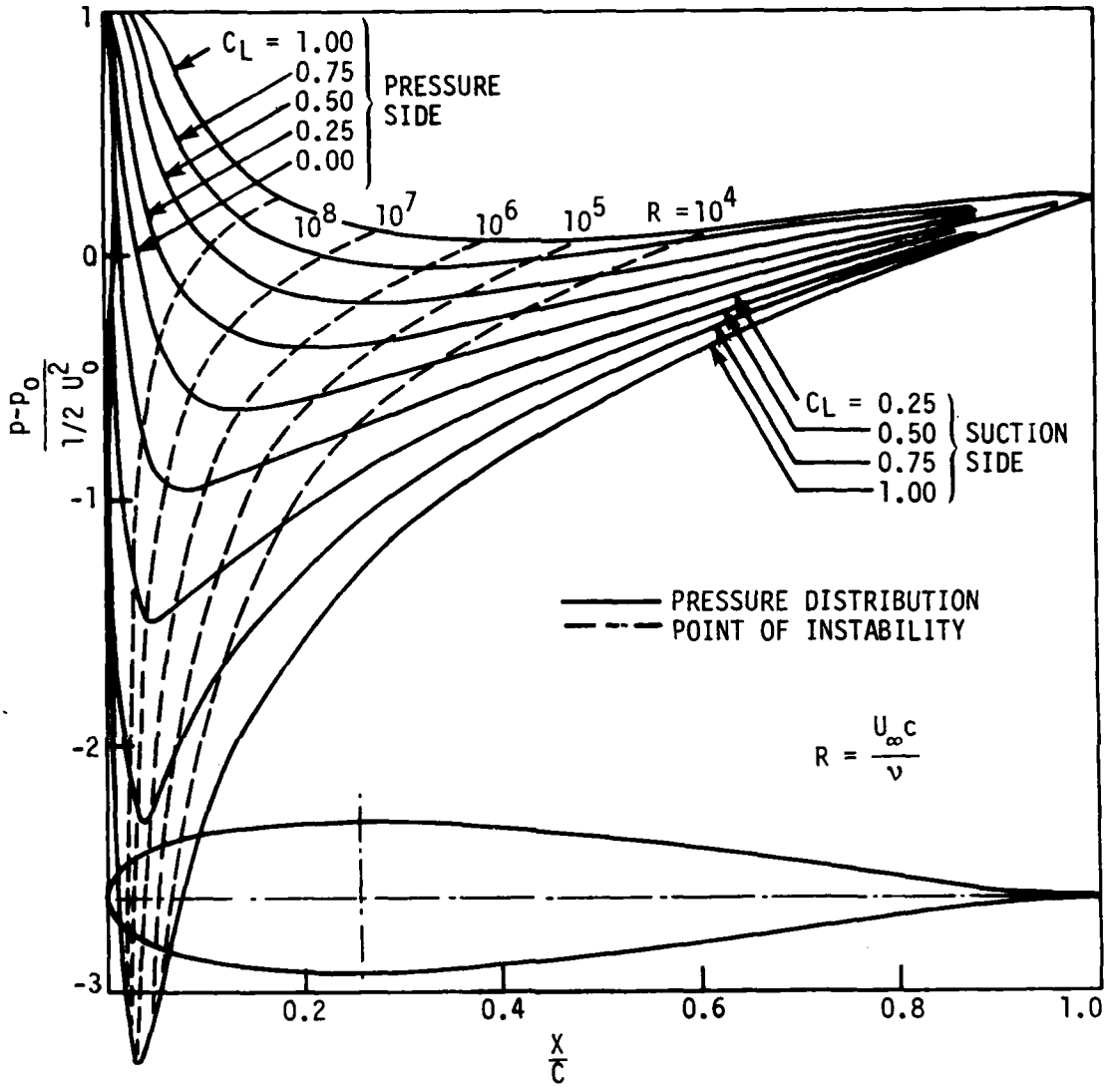

Fig. 1. Pressure distribution and position of instability on an airfoil showing Reynolds number and lift coefficient effects from Schlichting (5).

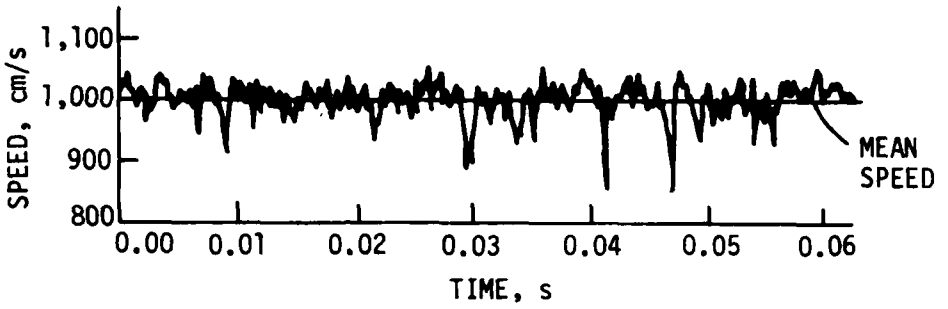

(a)

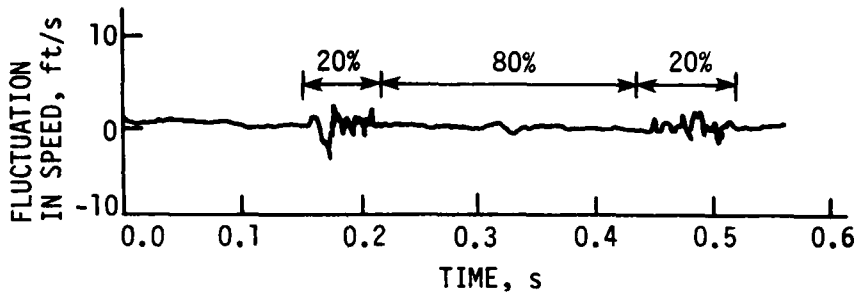

(b)

Fig. 2. Hot wire measurements showing intermittent turbulent fluctuations from White (1).

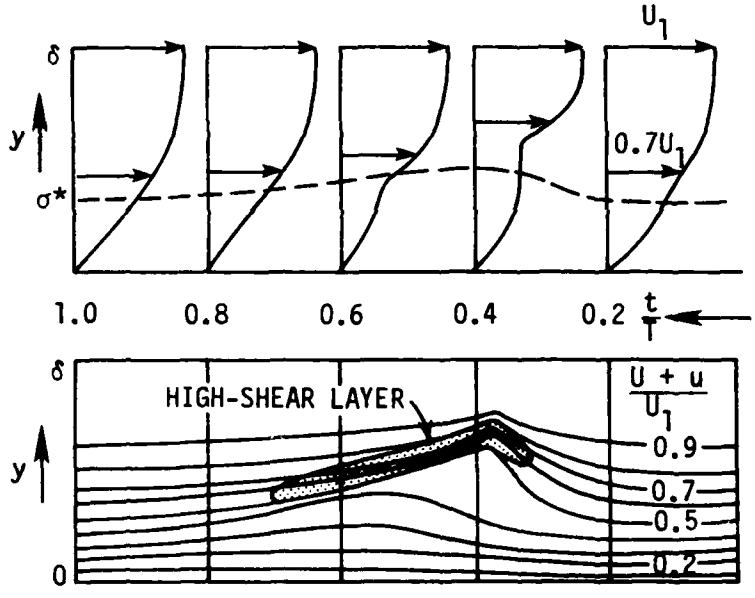

Fig. 3. Instantaneous velocity profiles and contour of high-shear layer in the boundary layer at first appearance of spikes, from Tani (12).

Walker (8) used a stethoscopic technique to detect the acoustic emissions from the formation of turbulent spots. The formation of turbulent spots constituted the initial stage of transition in his boundary layer studies on compressor blades. Walker also employed a China-clay drying technique.

2.2. Qualitative Description of Transition Initiation

The transition process generally results from a buildup of disturbances in the boundary layer. According to Mack (9), transition results from external disturbances interacting with the boundary layer either directly or through instability waves. Reshotko (10) describes transition as the non-linear response of the laminar boundary layer to a random forcing function, i.e., infinitesimal disturbances. Roudebush and Lieblein (11) state that transition results from finite amplitude disturbances such as freestream turbulence or surface roughness, or from the exponential growth of small instability waves.

2.2.1. White's Description

White (1) describes the mechanism of this process qualitatively and is generally supported by many other investigators in boundary layer theory. His six step process consists of the following steps as the flow develops downstream.

1. Initiation of unstable two-dimensional Tollmien-Schlichting (T-S) waves. This is the period of initial instability developing from the laminar boundary layer as predicted from linear stability theory. Linear stability theory locates the critical

Reynolds number where the T-S waves begin to grow. The T-S waves exhibit fairly long wavelengths, with a minimum wavelength of 6δ. These waves travel at speeds of less than 0.4 U, as predicted by linear stability theory. Obremski, Morkovin, and Landhal (7) state that this linear region of the flow ceases to exist when the velocity fluctuation exceeds two percent of the freestream velocity.

2. Development of three-dimensional instability. The growth of the T-S waves begins to vary in the spanwise direction. Walker (8) suggests that the Tollmien-Schlichting waves may possess some slight three-dimensionality which becomes amplified by secondary flows or turbulence in the freestream. Next, according to Tani (12), the wave amplitude develops a spanwise component which increases as the flow progresses downstream. A spanwise velocity component, which varies with time and spanwise distance, also develops. This, in turn, initiates the development of streamwise vortices.
3. Development of a peak-valley system. The streamwise vortices begin to concentrate locally and form S-shaped eddies in the spanwise direction (8). Knapp and Roache (3) call this process "thatching." A periodic streamwise vorticity system develops into counterrotating vortices. Alternating velocity "peaks" and "valleys" form in the spanwise direction with maximum velocity fluctuations at the peaks. According to Tani, a mean velocity defect is produced at the peaks, and a velocity excess at the valleys.

4. Shear layer development and vortex breakdown. Large shear areas develop in the boundary layer (see Figure 3) caused by a concentration of vorticity at the peaks. An inflection point develops instantaneously and periodically in the velocity profile of this region. Once the shear layer forms, the vortices, which have become stretched in an S-shape in the spanwise direction, begin to break down. According to White (1), these vortices continue to break down into smaller and smaller vortices until all periodicities disappear and random fluctuations set in. van Driest and Blumer (14) regard this step as the beginning of transition.

5. Formation of turbulent spots. When randomness sets in, turbulent spots begin to burst forth near the peaks of the vorticity. These spots develop into the familiar three-dimensional turbulent spots. Obremski and Fejer (28) divide this growth into two modes: a "creative" mode characterized by accelerating growth, and a "convective" mode characterized by constant growth. Such factors as adverse pressure gradient or heat transfer can promote the creative growth mode and, consequently, speed up the transition process. A number of authors, including Walker (8), Forest (15), and Dunham (6), regard this step as the actual beginning of transition. Obremski, Morkovin and Landhal (7) have noted that turbulent spots form when u'/U exceeds 12%. Along with Tani (12), they note that non-linear regions act independently of Reynolds number.

6. Coalescence of spots into turbulent flow. The flow between the turbulent spots is still laminar. Hot-wire measurements in this region will show intermittent turbulence, increasing in the x direction until complete turbulent flow forms. In this region, the turbulent boundary layer equations become more applicable. From the turbulent boundary layer viewpoint of Kline (43), energy transfer occurs from the mean flow to the boundary layer fluctuations. The extent of turbulence production should be affected by the local stability of the flow (inflection point in the velocity profile). Turbulence production is influenced by such factors as pressure gradient and surface curvature. The entire process from step 1 through step 6 is shown in Figure 4.

Knapp and Roache (13) add an interesting observation based on flow visualization studies on an axisymmetric ogive cylinder. A relaminarization process occurs intermittently in the boundary layer after turbulent spot formation. The breakdown of the thatched vortices into smaller vortices causes an instantaneous localized favorable pressure gradient of sufficient magnitude to induce a brief flow relaminarization. This period is of short duration, and the vortex breakdown process continues immediately afterwards.

2.2.2. Morkovin's Transition System

The entire process described above indicates the highly unsteady, three-dimensional character of nominally two-dimensional flat plate flow. Flow conditions such as pressure gradient, surface roughness,

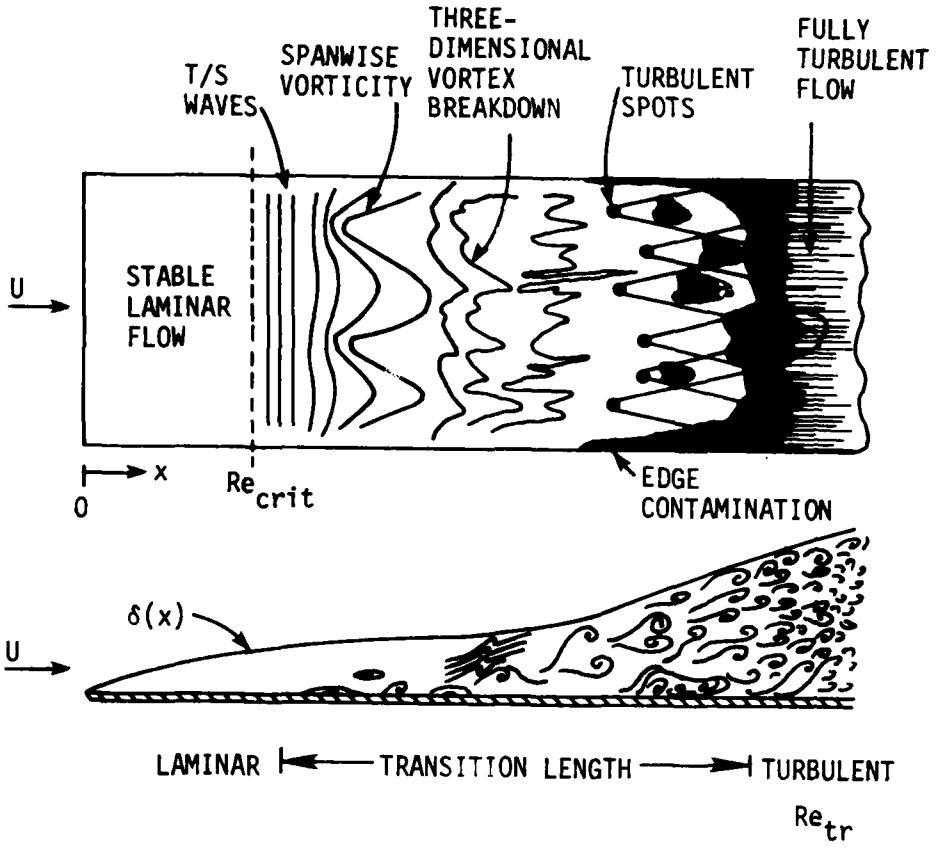

Fig. 4. Transition process on a flat plate from White (1).

three-dimensionality, and heat transfer act upon various segments of the process to either amplify or damp the disturbances. Morkovin (2) describes a more generalized concept to include parametric effects of the flow environment. His proposed system is based on amplification of the disturbances of linear stability theory. The diagram in Figure 5 describes this system, illustrating the freestream characteristics acting as an oscillator, providing input disturbances to an "operation" amplifier. The flow environment, composed of the mean boundary layer properties of pressure gradient, surface roughness, heat transfer, etc., determines the characteristics of the amplifier. This "operation" amplifier produces three-dimensional development of the disturbances and subsequent vortex stretching in the spanwise direction. Eventually this leads to turbulent spot production and subsequent transition.

Morkovin also introduces the concept of "receptivity" to describe the effects of the flow environment on amplification of disturbances. This concept accounts for the scale, range, and frequency of disturbances similar to those in the Tollmien-Schlichting instability waves. The disturbance environment forces transition to occur. Unfortunately, the exact nature of this complex environment is rarely comprehensible; consequently, an accurate prediction of the operation amplifier is often difficult.

Reshotko (10) describes receptivity as the response of the laminar boundary layer to external forced oscillations of a frequency and speed comparable to those of the instability waves. The "signature" of the external flow must be known. Obremski, Morkovin, and Landahl (7) describe receptivity as a transfer function of the disturbances which

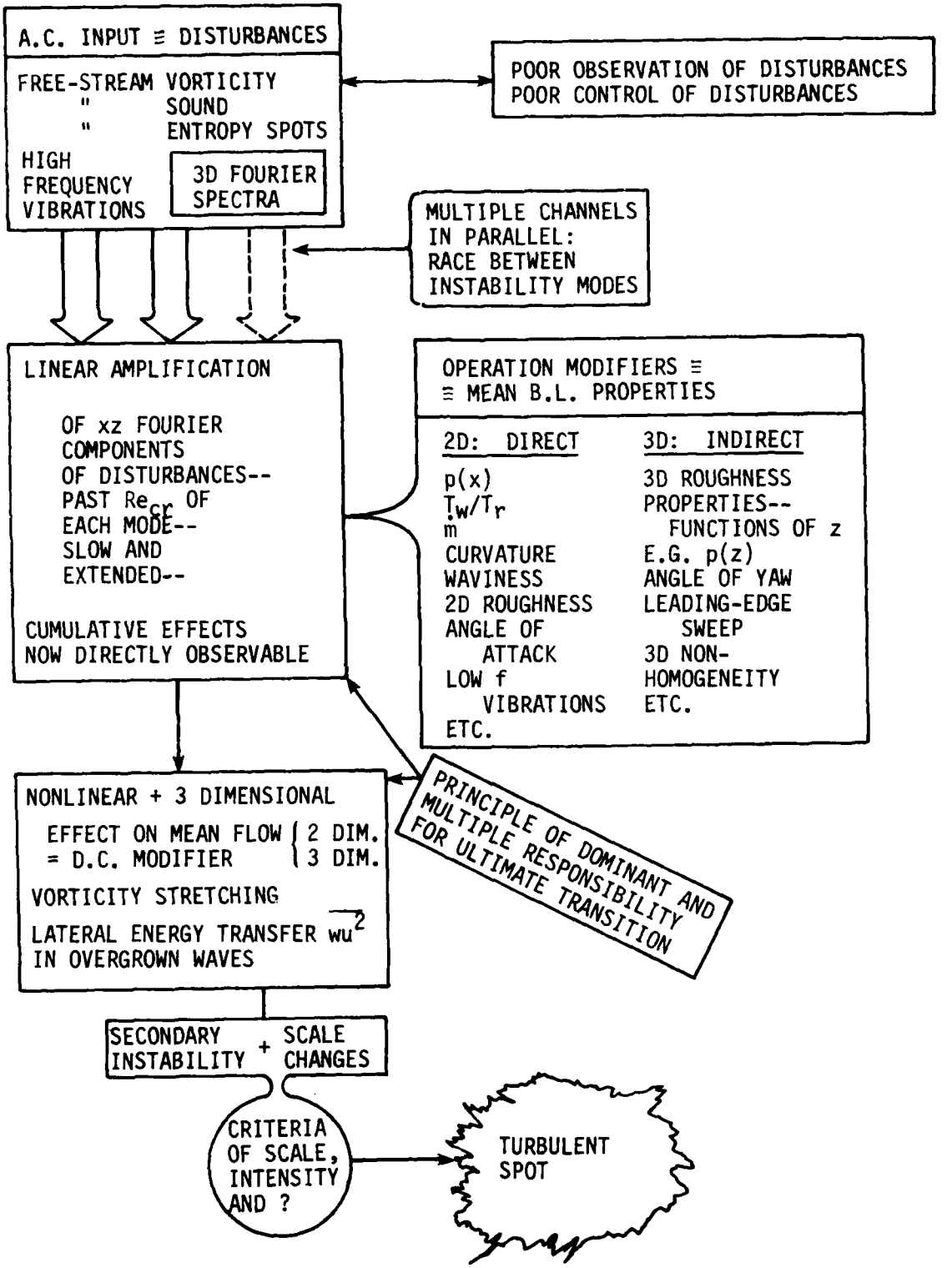

Fig. 5. Description of transition system from Morkovin (2).

match the T-S wave spectra. They also state that determination of the disturbance environment is a formidable job.

The concept of "bypasses" is also proposed, which allows the input and amplification of relatively high-amplitude disturbances such as freestream turbulence and flow unsteadiness. The bypass mechanism permits turbulent spot formation without Tollmien-Schlichting amplification. An example of this is the transition in pipe flow, where stability analysis does not predict transition. Another example is two-dimensional Poiseuille flow in which transition occurs ahead of the flow instability point.

2.3. General Stability Theory

The appearance and growth of Tollmien-Schlichting waves, as discussed in step 1 above, can be mathematically predicted with reasonable accuracy by linear stability theory--the only viable theory of the transition process. According to Mack (9, 16), the mechanism by which instability waves are produced is unknown. However, transition prediction and experimental verification depend on the observer's ability to trace the origin of the instability. Stability theory cannot predict the location of transition, but it can establish unstable velocity profiles, isolate unstable frequencies, and evaluate parametric influences.

Stability computations have been conducted on Blasius profiles by Brown (1959), on Falker-Skan profiles by Wazzan, Okamura, and Smith (1963), and on plane Poiseuille flow by Shen (1954). The experiments of Dryden, Schubauer and Skramstad in the early 1940s at the National Bureau of Standards verified predictions of stability theory for Blasius flow.

2.3.1. Linear Stability Theory

The following discussion is based on the writings of Schlichting (5), White (1), Mack (9, 16), and Obremski, Morkovin, and Landahl (7). The cornerstone of stability theory is the Orr-Sommerfield equation, which is derived from the Navier-Stokes equation for two-dimensional flow. It assumes small disturbance of the mean boundary layer velocity U(y), thus permitting a linear solution of the Navier-Stokes equation. Next, the unsteady stream function is written for the single oscillation of the disturbance.

$$\psi(x,y,t) = \phi(y)e^{i(\alpha x-\beta t)} \tag{1}$$

where $\alpha = 2\pi/\lambda$ represents the wave number, and β is a complex number:

$$\beta = \beta_r + i\beta_i \tag{2}$$

We now define the complex quantity

$$C = \frac{\beta}{\alpha} = C_r + iC_i \tag{3}$$

where C_r represents the wave propagation velocity and C_i represents the degree of damping or amplification from the unsteady stream function. The oscillating components of the boundary layer may be written and substituted into the Navier-Stokes equation. The result is the fourth order ordinary differential equation for the disturbance amplitude $\phi(y)$:

$$(U - C)(\phi'' - \alpha^2\phi) - U''\phi = \frac{-i}{\alpha Re_\delta}(\phi'''' - 2\alpha^2\phi'' + \alpha^4\phi) \tag{4}$$

where the primes denote differentiation with respect to the dimensionless coordinate y/δ. This is an eigenvalue problem. If a temporal stability

analysis is required to determine the time-dependent amplification of the disturbance, then the four independent parameters of equation (4) are α, Re_δ, C_i and C_r. If a spatial analysis is required to calculate the disturbance growth in the x direction, then the parameters are Re_δ, α_r, α_i, and C. This distinction is summarized as follows.

Temporal stability		Spatial stability	
α	real	α	complex
C	complex	C	real
$C_i > 0$	damped	$\alpha_i > 0$	damped
$C_i < 0$	amplification	$\alpha_i < 0$	amplification

The eigenvalue problem is solved by numerical integration of the Orr-Sommerfeld equation which yields one eigenfunction $\phi(y)$, one complex eigenvalue $C = C_r + iC_i$, for each pair of α and Re_δ. Solution of this equation yields phase velocity, amplitude ratio, overall growth, unstable frequencies, and $Re_{\delta crit}$. The critical Reynolds number is the minimum Reynolds number on the neutral stability curve $C_i = 0$, below which no disturbances of any wavelength will be amplified. This number is used to locate the position of initiation of the Tollmien-Schlichting waves. Typically, the most unstable wave numbers decrease as the square root of Re_δ for increasing Reynolds number. The effect of pressure gradient can be evaluated by determining the neutral stability curve and $Re_{\delta crit}$ using Falkner-Skan profiles.

Several general theorems have been deduced from inviscid stability theory, which assumes large values of Reynolds number. This leads to a second order ordinary differential equation from the Orr-Sommerfeld

equation. Two of the theorems which have application to viscous flows are

> Theorem [Tollmien (1929)]--It is sufficient for instability of boundary layer profiles that the velocity profile have an inflection point.
>
> Theorem [Rayleigh (1880)]--The phase velocity of an amplified disturbance must always lie between the minimum and maximum values of U(y).

Adverse pressure gradients in two-dimensional flows typically induce inflection points in viscous velocity profiles. The speed of propagation of amplified disturbances (phase velocities) is less than 0.4 U.

2.3.2. Types of Flow Instabilities

Schlichting (5) discusses flow instabilities over curved surfaces. A change in sign of the expression

$$\frac{d^2u}{dy^2} + \frac{1}{R}\frac{du}{dy} \qquad (5)$$

indicates instability on curved walls. R denotes local radius of curvature with $R > 0$ denoting a convex and $R < 0$ denoting a concave wall. Centrifugal forces on convex walls have a stabilizing effect, while centrifugal forces on concave walls have a de-stabilizing effect.

On concave surfaces, a primary instability in the form of Görtler vortices develops. Tani (12) indicates that these vortices cause a spanwise variation in boundary layer thickness. Wortmann (17), who conducted flow visualization tests with water, describes this instability as counter-rotating streamwise vortices in the spanwise direction with alternating inflection-type velocity profiles. Progressing downstream,

the Görtler vortices oscillate causing a lateral fluctuation of the velocity profile followed by the formation of turbulent spots. Dryden (18) suggests that this type of instability dominates over Tollmien-Schlichting waves when $\delta^*/R > 0.00013$.

2.4 Laminar Separation

Laminar separation is important in the fluid mechanics of airfoils and compressor blading. There is, in a sense, a "race" between laminar separation and "natural" transition on the suction surfaces. Roudebush and Lieblein (11) point out that transition makes axial flow compressors possible since the resultant turbulent boundary layer is less prone to separation than the laminar boundary layer.

The initiation of laminar separation is independent of Reynolds number. It depends almost solely on the pressure gradient and occurs when the pressure gradient parameter falls below the value proposed by Thwaites:

$$m_\theta = \frac{\theta^2}{\nu} \frac{dU}{dx} < -0.082 \qquad (6)$$

This criterion is used by Walker (8), Seyb (19), and Roberts (20). Dunham (6), and others, use -0.09 as a criterion. Citavy and Norbury (21), and Kiock (22), report that increasing turbulence intensity of the freestream moves the separation point downstream. Their observations are based on cascade tests involving artificially induced turbulence. Tani (12) reports that separation bubble formation is possible only when $Re_{\delta^*} > 500$ on airfoils, a claim verified by Owen and Klanfer.

Laminar separation is undesirable since it causes high losses. It is experimentally indicated by a sharp increase in momentum thickness, θ, and a sharp decrease in shape factor, H (11). According to Roberts (20), separation is likely in laminar flow for adverse pressure gradient, smooth surface, and low Tu levels. Five possible events can occur in relation to potential separation:

1) natural transition (no separation)
2) short bubble formation
3) long bubble formation
4) turbulent separation
5) complete separation; no reattachment

The two significant events for transition studies are the short and long bubble formation. Roberts (20) differentiates between the two concepts when he states that a short bubble has a negligible effect on the streamwise pressure distribution, while a long separation bubble affects the exterior freestream flow and the resultant pressure distribution, including location of the pressure peak. Laminar separation, in general, causes an initially thicker turbulent boundary layer than natural transition.

A summary of the laminar separation mechanism will be presented, based on compressor tests by Walker (8, 23), cascade test data compiled by Roberts (20), and isolated airfoil experiments by Gault (24). A laminar separation diagram based on the work of Walker (8) is shown in Figure 6.

After laminar separation occurs, a free shear layer forms between the top of the boundary layer and the bubble. In the bubble itself, a

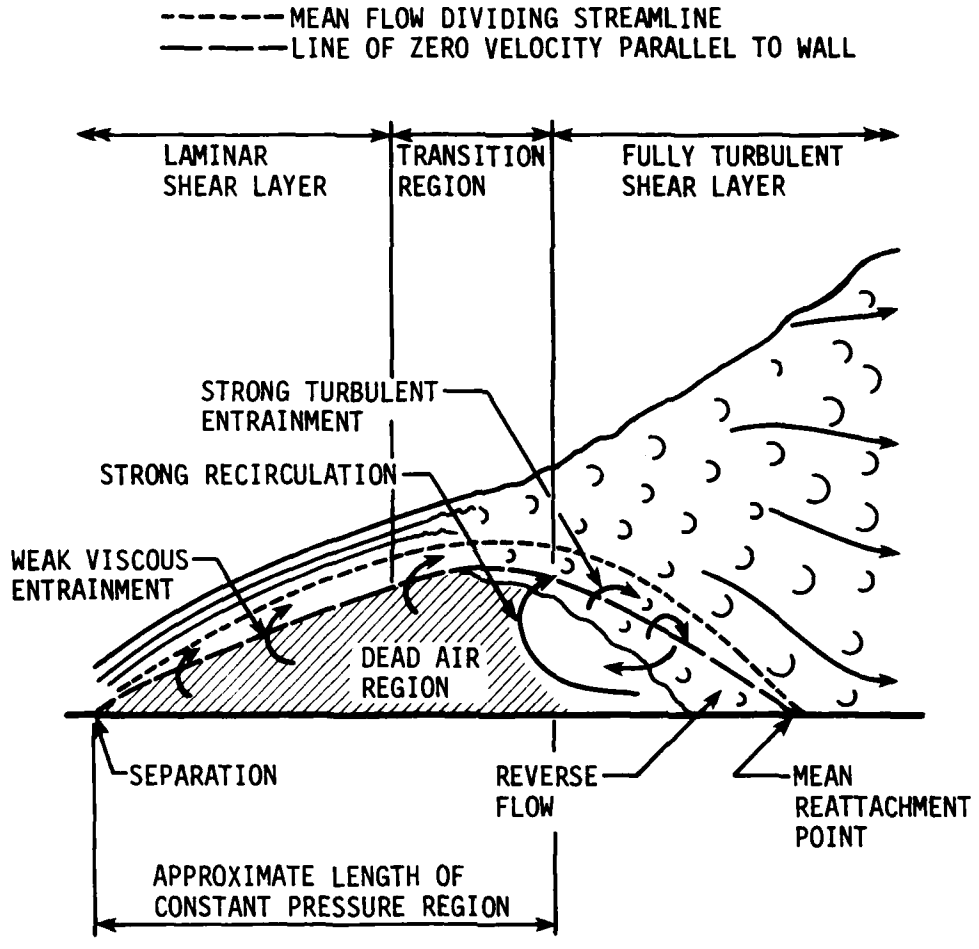

Fig. 6. Flow mechanism of a two-dimensional laminar separation bubble from Walker (8).

small region of reverse flow gives rise to a "dead air" region of constant streamwise pressure. Dryden (18) notes that laminar shear layers are unstable, encouraging transition. Tani (12) suggests that this occurrence can be approximated by the following formula:

$$l_1 = 100\delta_s^* \tag{7}$$

Horton (42) proposes the following criterion for airfoils:

$$l_1/\theta_s = 4 \times 10^4/Re_{\theta,s} \tag{8}$$

where $Re_{\theta,s}$ is the momentum thickness Reynolds number at the separation point. Tani and Roberts suggest that transition occurs at a particular point while Walker (8) defines a finite length region. In the transition region, a turbulent shear layer forms, a layer containing more diffusion energy than the laminar shear layer. Subsequent reattachment occurs and the amount of reverse flow in the bubble increases. Gault characterizes the turbulent shear layer as a region of high vorticity which reattaches the flow. Horton (42) determined that reattachment occurs under the following condition:

$$\frac{\theta}{U}\frac{dU}{dx}_R = -0.0059 \tag{9}$$

where R denotes the reattachment point. Horton also presents a semi-empirical equation for determining the length of the transition region, l_2.

Pressure rises abruptly at the end of the transition region. If a long bubble forms, the turbulent shear layer must do more diffusion to reattach, causing lower pressure recovery, reduced minimum pressure on

the suction surface, and reduced circulation.

Theoretically, separation is indicated by a zero wall shear stress. ln unsteady flows in turbomachinery, this condition may be difficult to locate experimentally.

2.5. General Prediction Methods

A number of transition prediction criteria have been advanced based on flat plate studies. They generally consist of experimental correlations, but some are based on linear stability theory. A more detailed treatment of these methods is presented by Walker (8), Morkovin (2), and Hall and Gibbings (4).

2.5.1. The van Driest and Blumer Method

In the model proposed by van Driest and Blumer (14), a vorticity Reynolds number is defined:

$$T_r = \frac{y^2}{\nu} \frac{du}{dy} \tag{10}$$

where du/dy is measured at the point of maximum vorticity, based on the observation that the ratio of local inertial stress to local viscous stress must reach a limiting value at transition. The resultant vorticity Reynolds number will reach a limiting value at some value Re_x, which must be determined experimentally. Effects of freestream turbulence, surface roughness, and adverse pressure gradient will increase the value of the local vorticity Reynolds number and reduce the transition Reynolds number. A curve fit was applied to the data of Dryden, Hall and Hislop, and Schubauer and Skramstad; the correlation was then extended to the

Pohlhausen velocity profiles to account for the effect of pressure gradient:

$$\frac{9860}{Re_{\delta,t}} = 1 - 0.0485\ \lambda + 3.36\ Re_{\delta,t}\left(\frac{u'}{u_\delta}\right)^2 \qquad (11)$$

2.5.2. The Crabtree Method

Crabtree's method (25) establishes a correlation of $Re_{\theta tr}$ vs. $m_{\theta tr}$ for experimental data at low turbulence, Tu < 0.2%. He uses both flat plate and isolated airfoil data, and locates the laminar separation region based on Thwaites criteria. Crabtree defines transition as the limit of existence of laminar flow. Consequently, according to Hall and Gibbings (4), he is actually locating the end of transition. To use this method, it is necessary to calculate the boundary layer growth at each x station and plot Re_θ vs. m_θ. Transition is predicted at the intersection of the curve shown in Figure 7.

2.5.3. The Granville Method

Hall and Gibbings (4) consider Granville's method very similar to Crabtree's. Granville, however, plots $(R_{\theta tr} - R_{\theta crit})$ vs. $\bar{m}_\theta$, where $\bar{m}_\theta$ is the average pressure gradient parameter within the instability region. In other words, Granville's method is basically a replotting of Crabtree's data. Granville studied the effect of freestream turbulence and showed that $Re_{\theta,tr}$ approaches a value of 180 as Tu exceeds 5%.

2.5.4. The e^n Method

This method is based on a strict extension of stability theory computations. The ratio of the disturbance amplitude to the initial

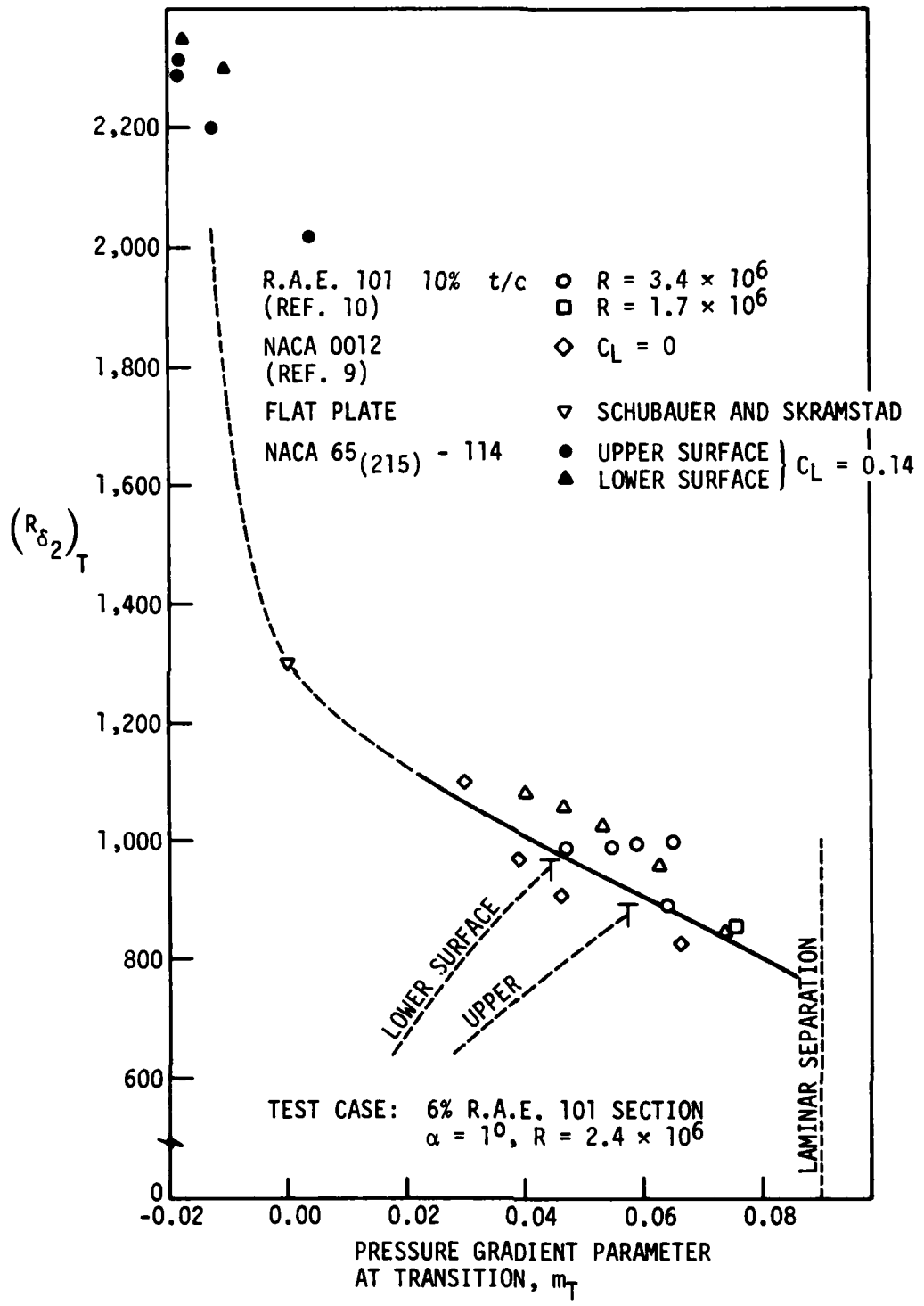

Fig. 7. Transition prediction data correlation from Crabtree (25).

value is computed. Van Ingen (29) computed these ratios from stability diagrams and compared them to experimental results on isolated airfoils. The amplification exponent is, by definition,

$$n = \ln \frac{A}{A_o} \tag{12}$$

where A_o is the amplitude of the initial disturbance. Van Ingen maintained that stability theory is good for predicting the early stages of transition. Basing his method on airfoil experiments, he proposed a value of n = 7 or 8. Smith and Gamberoni recommended n = 9. Van Ingen did note that the method becomes inaccurate in adverse pressure gradients near the point of laminar separation.

All of the methods mentioned thus far require computing the boundary layer variables δ, θ, δ^*, Re_θ at each station and comparing them to the critical values or transitional values at that station.

2.5.5. The Hall and Gibbings Method

Hall and Gibbings (4) present a general criterion for locating transition based on the data correlation of flat plate and concave surface studies. Their correlation (see Figure 8) is useful since the data represent different values of pressure gradient. Compressor blade, cascade, and isolated airfoil data involve variable pressure gradient in the streamwise direction.

Hall and Gibbings define the transition location as the point of minimum pressure. As previously mentioned, this is not a very accurate method because of the Reynolds number effect.

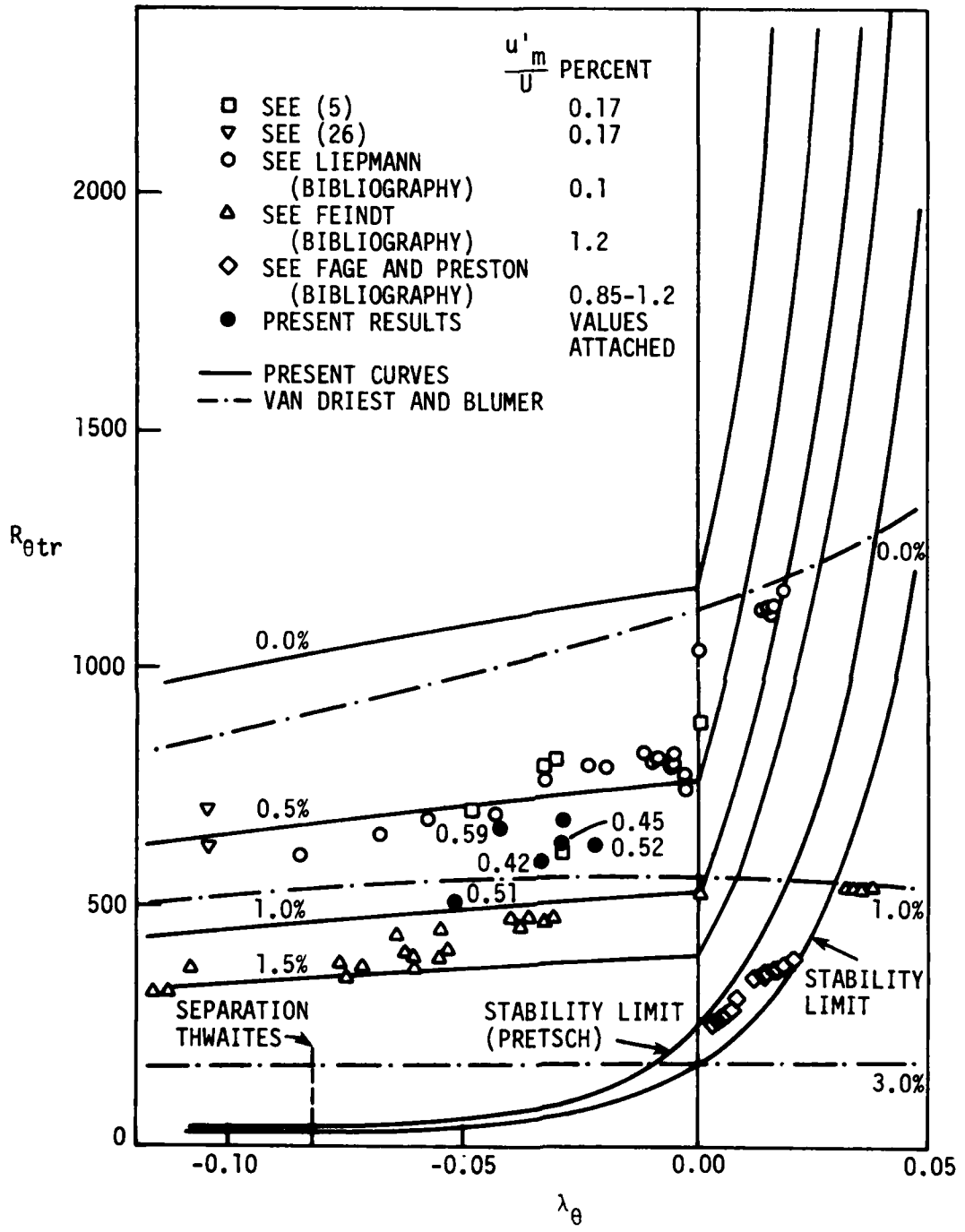

Fig. 8. Transition prediction data correlation from Hall and Gibbings (4).

3. PARAMETRIC EFFECTS ON TRANSITION

In this section, parameters which affect the transition process will be examined with emphasis placed on those variables having particular application to flow thru axial flow compressors, cascades, and isolated airfoils. A review of the pertinent literature revealed that while extensive tests have been conducted on individual effects, combined effects have not been adequately investigated.

The major influences on transition are the pressure gradient, turbulence intensity, and surface roughness, though surface curvature, heat transfer, and acoustic disturbances also have some effect. The relative importance of each parameter depends on the particular flow situation.

3.1. The Effect of Pressure Gradient

The freestream pressure gradient has the greatest effect on transition. Walker (8) points out that pressure gradient effects account for about one-half of all combined effects for two reasons. First, the instability point Re_{δ^*i} is influenced strongly by pressure gradient; second, the distance between transition and instability ($Re_{\delta^*tr} - Re_{\delta^*i}$) is affected. In this region, the amplification factors are altered by pressure gradient.

The external pressure gradient for airfoils and airfoil cascades can be calculated by several techniques using iterative inviscid/boundary layer computation. These techniques are summarized in a review by Hansen (27).

The effect of pressure gradient is stronger on the instability Reynolds number than on the transition Reynolds number. White (1) obtained the following approximations for Pohlhausen profiles:

$$Re_{\delta^*crit} \cong 520\ e^{0.6\lambda} \tag{13}$$

$$Re_{\delta^*tr} \cong 2900\ e^{0.08\lambda} \tag{14}$$

Reshotko (10) points out that a favorable gradient has a stronger effect on instability than an adverse pressure gradient. This phenomenon is illustrated for Falkner-Skan laminar profiles in Figure 9. The overall effect of pressure gradient on transition is shown in Figure 10.

Adverse pressure gradients tend to act on the step 3 mechanism of transition. The S-shaped spanwise vortices show less tendency to "thatch" and are more rounded, indicating less vortex stretching and more compression. The compression of these vortices causes more rapid breakdown (13) and promotes the "creative" growth mode of turbulent spot production (28).

3.2. The Effect of Freestream Disturbances

The effects of freestream turbulence are perhaps the most controversial aspect of boundary layer transition. Conflicting ideas have arisen regarding their effect on stability and on final transition. Freestream turbulence in axial flow turbomachinery consists of two components: random fluctuations of the mean flow and flow unsteadiness due to the stator and rotor wakes. It is worthwhile to consider the effect of unsteadiness effects separately.

3. PARAMETRIC EFFECTS ON TRANSITION

In this section, parameters which affect the transition process will be examined with emphasis placed on those variables having particular application to flow thru axial flow compressors, cascades, and isolated airfoils. A review of the pertinent literature revealed that while extensive tests have been conducted on individual effects, combined effects have not been adequately investigated.

The major influences on transition are the pressure gradient, turbulence intensity, and surface roughness, though surface curvature, heat transfer, and acoustic disturbances also have some effect. The relative importance of each parameter depends on the particular flow situation.

3.1. The Effect of Pressure Gradient

The freestream pressure gradient has the greatest effect on transition. Walker (8) points out that pressure gradient effects account for about one-half of all combined effects for two reasons. First, the instability point Re_{δ^*i} is influenced strongly by pressure gradient; second, the distance between transition and instability ($Re_{\delta^*tr} - Re_{\delta^*i}$) is affected. In this region, the amplification factors are altered by pressure gradient.

The external pressure gradient for airfoils and airfoil cascades can be calculated by several techniques using iterative inviscid/boundary layer computation. These techniques are summarized in a review by Hansen (27).

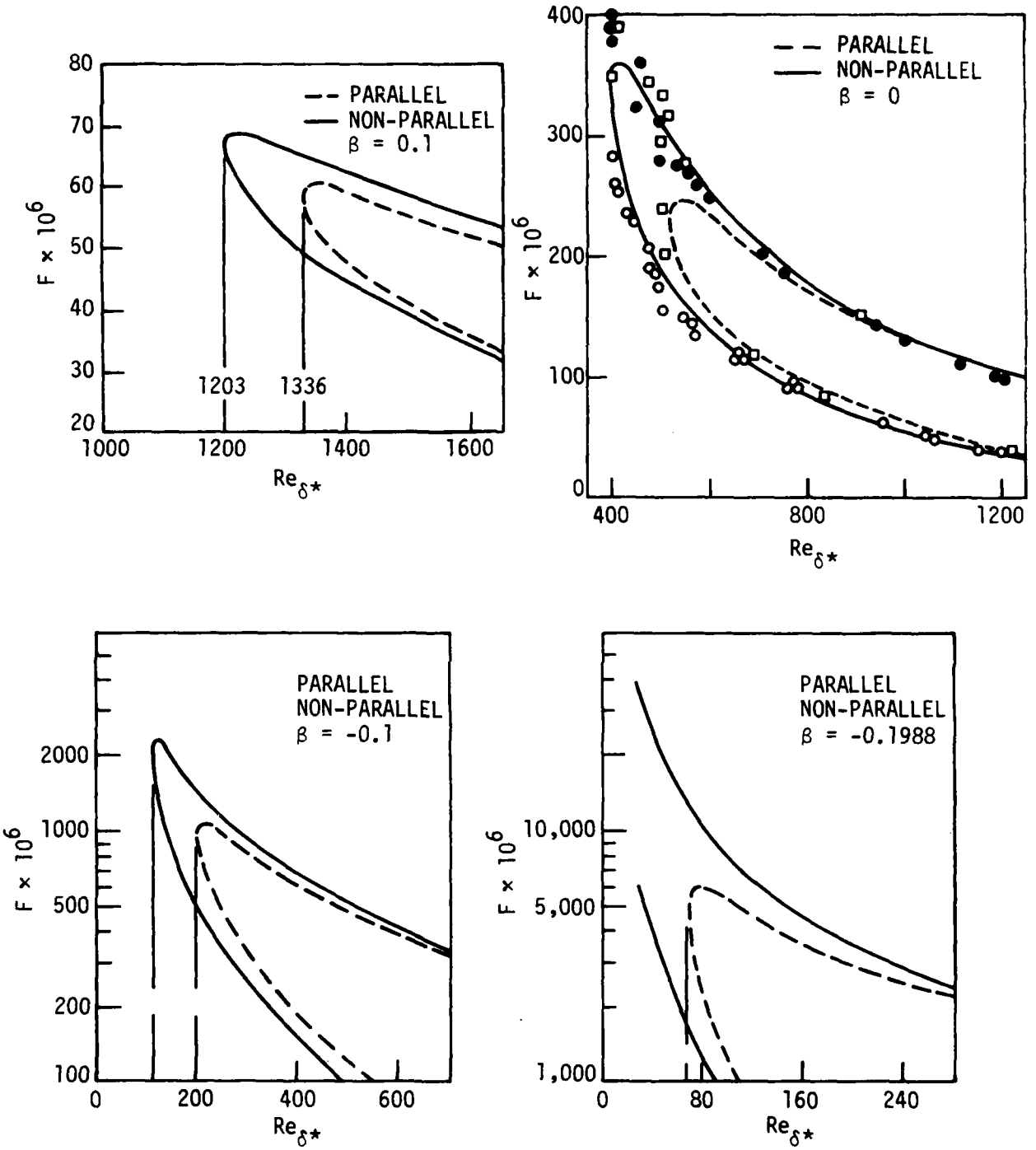

Fig. 9. Neutral stability diagrams for Falkner-Skan flows showing the effect of pressure gradient from Reshotko (10). Parallel flow indicates a streamwise component of the mean flow velocity. Non-parallel indicates existence of a vertical component.

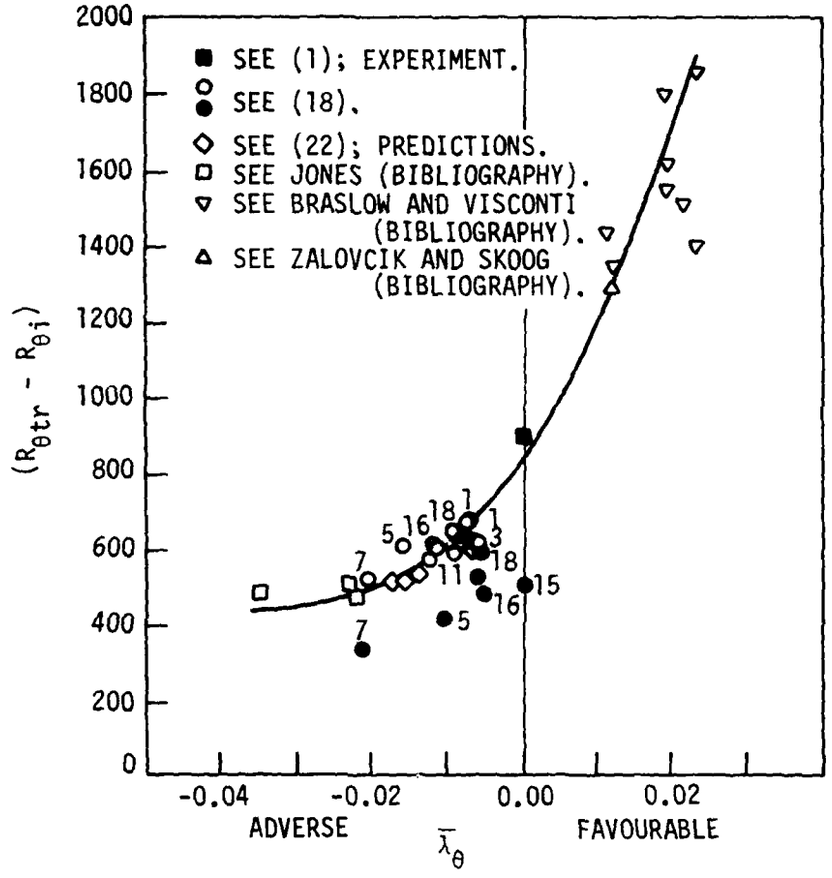

Fig. 10. Transition data correlation showing effect of pressure gradient from Hall and Gibbings (4). $\bar{\lambda}_\theta$ denotes the average pressure gradient parameter over the instability region.

3.2.1. The Effect of Flow Unsteadiness

Data on periodic unsteadiness comes principally from Obremski and Fejer (28), who conducted flat plate wind tunnel tests with oscillating shutter blades. They defined transition as the location where the intermittency factor $\gamma > 0$. Frequency of the oscillations ranged from 5 to 60 Hz, with Tu < .2%. They defined a "non-steady" Reynolds number

$$Re_{Ns} = \frac{L^*\Delta U}{2\pi\nu} \tag{15}$$

where L* is a characteristic length parameter. If this value exceeded 27,000, the transition process was periodic; if less than 25,000, the transition was "aperiodic." Generally, unsteadiness had little contribution in favorable pressure gradients if $\Delta U/U < 0.20$. For adverse pressure gradients, $Re_{Ns} > 6{,}000$ indicated periodicity.

Downstream, turbulent bursts appear in the troughs of the unsteady, instantaneous velocity trace. The flow unsteadiness appears to promote the "creative" mode of turbulent spot growth with subsequent reduction in transition lengths. Steady flow favors the "convective" mode of spot development.

Dzung (29) also points out that unsteady flow generates a "starting vortex" on each cycle because of the time-varying circulation. This vortex is convected downstream to the next set of blade rows. Walker (8) reinforces these observations in his compressor studies and adds that when Re_{Ns} exceeds the critical value, the spots appear in ribbon-like form in the spanwise direction.

Obremski and Fejer also noticed a "calm" period after the passing of turbulent spots similar to the calm period observed by Roache and Knapp (13).

3.2.2. The Effect of Overall Turbulence Intensity

The turbulence intensity parameter Tu consists of two parts: a periodic flow unsteadiness term and a random velocity fluctuation term. According to the single-stage compressor test results of Evans (30), these quantities are of equal magnitude at design speed. The periodic unsteadiness frequencies are equal to the blade passing frequencies. Random fluctuations have frequencies in the range of 20 Hz to 20 KHz (22).

Using compressor data, Kiock (22) reports that turbulence increases rapidly from 1% to 10% through a three-stage compressor. Schlichting and Das (31) quote other sources showing an increase of 6 to 8% through multi-stage compressors. Laminar separation bubbles tend to increase the downstream freestream turbulence. Citavy and Norbury have observed a small decrease in the pressure coefficient distribution across the cascade chord as turbulence increases. This change may be due to changes in the laminar separation bubble or to the axial velocity ratio which was also varied.

Using cascade test data, Schlichting and Das (31) observed that as turbulence increased from 0.5% to 2% there was an increase in boundary layer momentum thickness across the cascade chord. They also observed a decrease in the shape factor. Little change was observed above 2% turbulence, indicating formation of a turbulent boundary layer. This effect was also observed by Schäffler (32).

Schlichting (5) presents a strong case for turbulence effects on transition in a zero pressure gradient. Figure 11 shows that turbulence has little effect on duration. Though stability aspects of turbulence are not fully understood, Obremski (7) feels that freestream turbulence

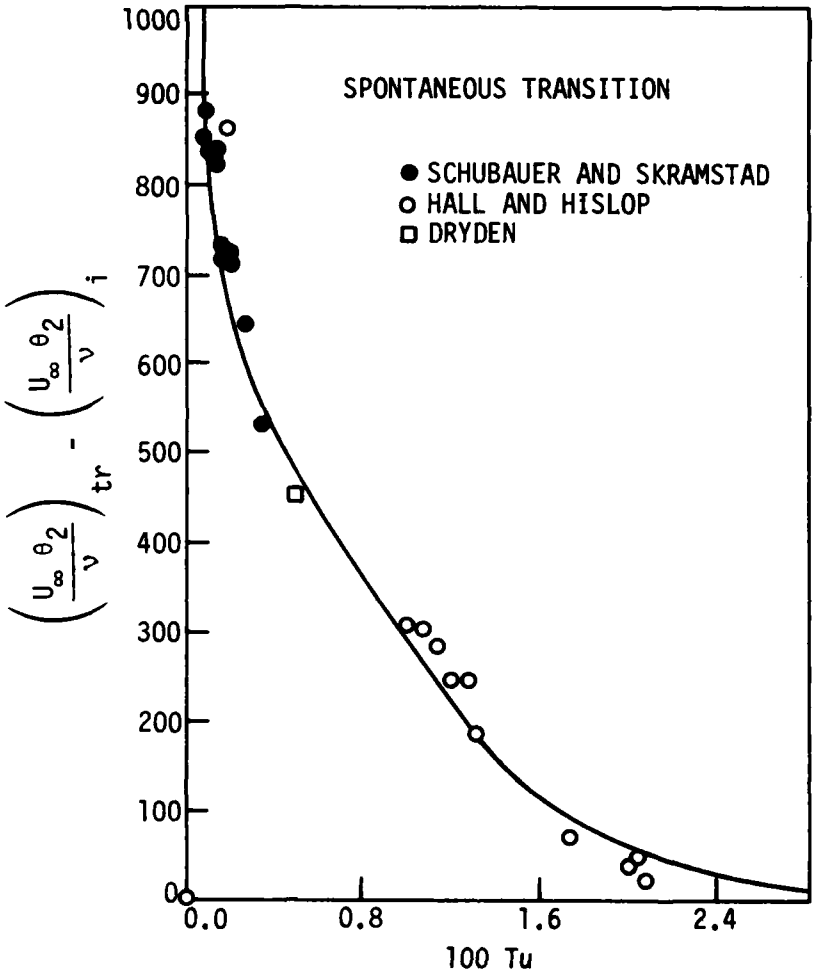

Fig. 11. Effect of freestream turbulence on the transition-instability location in a zero pressure gradient, from Schlichting (5).

may contain frequencies that are in the range of the Tollmien-Schlichting selective amplifier, while Morkovin (2), in his receptivity theory, allows turbulent disturbances of sufficient magnitude to "bypass" the Tollmien-Schlichting mechanisms altogether.

Rogler (33) presents the most cogent description of turbulence effects on stability. Freestream disturbances exist as vortex sheets, as rings and patches, or as wakes which convect into the boundary layer, an area of concentrated vorticity. A spatial analysis is conducted by writing a two-dimensional vorticity equation comprising convection, production, and diffusion terms for the boundary layer. The ingested freestream vorticity then induces three-dimensional velocities which generate additional boundary layer vorticity. A readjustment of the vorticity occurs, varying with time or distance. This disruptive activity induces forced oscillations with wavelengths in the range of the Tollmien-Schlichting amplifier followed by turbulent spot formation.

On a macroscopic level, Walker (8, 23) presents an entirely different view; he states that turbulence influences transition <u>indirectly</u> by directly modifying the pressure distribution. This assertion is supported by the cascade tests of Citavy and Norbury (21) and Kiock (22). Walker states that large scale freestream disturbances cause instantaneous changes in flow incidence which move the instantaneous suction peak and subsequent transition location. Walker then states that freestream turbulence has an effect on transition only if turbulence scale alters the pressure distribution and incidence, changes the initial amplification of neutral disturbances, or changes the amplification rate of all disturbances wavelengths. If none of these three conditions are met,

turbulence intensity is not expected to move up the transition location by more than 20% of $x_t - x_i$. Proponents of stability theory admit that the effect of turbulence intensity on instability is largely unknown (7); consequently, Walker's observations have some basis.

Horlock and Evans (34) attempted a theoretical treatment of turbulence intensity through use of the von Karman momentum integral equation. They suggest that additional terms be included in the equation and that the shear stress does not approach zero at the edge of the boundary layer. They propose the following relation:

$$\frac{\tau_\delta}{\tau_{wall}} = 4\ Tu \qquad (16)$$

3.3. The Effect of Surface Roughness

Much of the work on effects of surface roughness (12) has been conducted on two-dimensional tripwires or three-dimensional isolated elements, but it is not entirely clear which type of element applies to two-dimensional boundary layers.

First of all, Schäffler (32) states that it is difficult to characterize roughness because of the individual shape of peaks, the roughness peaks per unit of length, and the uniformity of roughness heights. The arithmetic average (AA) alone does not give a good description of the hydrodynamic characteristics. Schäffler defines the height parameter k as the difference between the 10 highest peaks and 10 deepest valleys in 100 μm of length. Thus, his roughness criterion is

$$Re_{k,crit} < \frac{k_s W}{\nu} = 100 \qquad (17)$$

for hydrodynamically smooth surfaces where W is the free stream velocity relative to the cascade.

For a single two-dimensional roughness element, Schlichting recommends

$$Re_{k,crit} = \frac{u_k k}{\nu} = 20 \qquad (18)$$

For an isolated three-dimensional element on two-dimensional flow, Tani (12) recommends

$$Re_{k,crit} = \frac{u_k k}{\nu} = 600 \qquad (19)$$

Tani also notes that pressure gradient has no effect on the value of $Re_{k,crit}$ in three-dimensional flow.

For distributed roughness, which is most applicable to actual turbomachinery flows, Schlichting (5) recommends

$$Re_{kcrit} = \frac{Uk_s}{\nu} = 120 \qquad (20)$$

Below this number, roughness has no effect on transition. In Figure 12 Schlichting's graph shows the effect of surface roughness and pressure gradient.

McDonald and Fish (3) present a convenient graph for distributed roughness based on the parameter k/δ^* (see Figure 13).

Referring to stability theory, Morkovin (2) states that roughness does not generate unsteady disturbances, but rather acts as a modifier

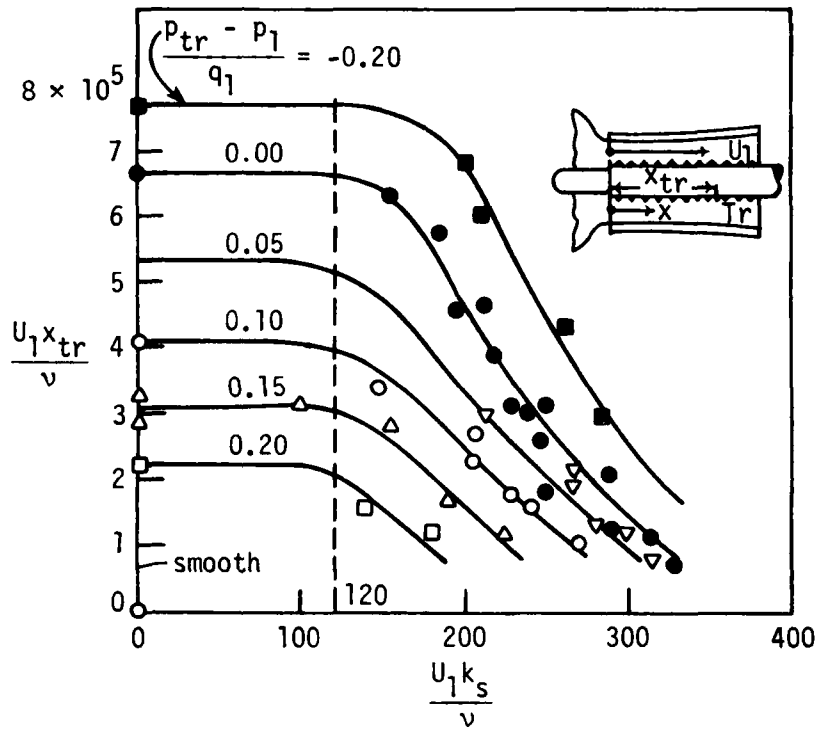

Fig. 12. Effect of surface roughness for various pressure gradients in incompressible flow from Schlichting (5).

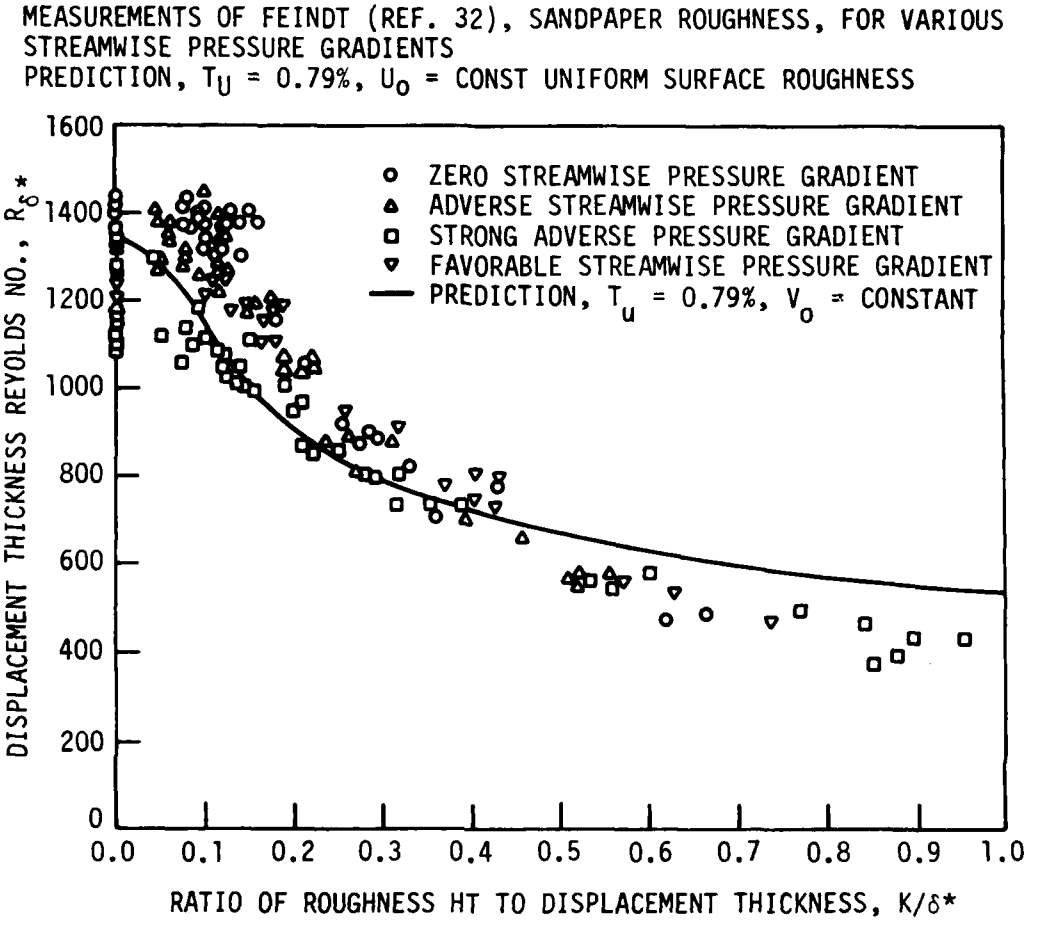

Fig. 13. Effect of distributed surface roughness on transition Reynolds number from McDonald and Fish (3).

to the instability waves. Dryden (18) takes the opposite view and argues that roughness elements generate disturbances through eddy production.

3.4. The Effect of Heat Transfer and Compressibility

In incompressible flow, heat transfer to the fluid causes Re_{crit} to decrease because of the dependence of viscosity on temperature; conversely, heat transfer from the fluid has a stabilizing effect. Schlichting (5) demonstrates mathematically, using the Navier-Stokes equation, how heat transfer to the fluid generates an inflection point in the velocity profile.

In compressible flow, a thermal boundary layer develops. Since the velocity at the wall is zero, the wall temperature approaches the stagnation temperature, as indicated by the recovery factor. For subsonic flow, this resultant heat transfer effect is slight up to a Mach number of 0.9.

At higher Mach numbers, however, local shock waves may be produced, generating a strong adverse pressure gradient and inducing transition (32). The study of transition in supersonic flows is of great interest in aeronautical engineering and a wealth of experimental data is available, though these applications are beyond the scope of this paper.

3.5. The Effect of Streamwise Surface Curvature

Centripetal forces generated on concave walls, such as pressure surfaces on airfoils, give rise to a primary flow instability called Görtler vortices which are characterized by alternating streamwise

vortices of opposite rotation and alternating inflection-type two-dimensional velocity profiles (secondary instability) (see Figure 14). In extensive flow visualization studies of these effects done by Wortmann (17), the vortices show an oscillating motion and the velocity peaks and valleys show a lateral movement. This instability destroys the symmetry of the vortices, and a fluctuation of the velocity profile occurs in all three planes, followed by turbulent spot formation.

Dryden (18) indicates that Görtler vortices become dominant if $\delta^*/r > 0.00013$. Tani (12) locates the point of instability through a Görtler number, and states the following stability limit:

$$G = R_{\delta^*}(\delta^*/r)^{1/2} > 1.2 \qquad (21)$$

Tani also presents a diagram (see Figure 15) to determine the transition Reynolds number.

On convex surfaces, centrifugal forces arising from the suction surface curvature exert a stabilizing influence on transition (5). If, however, δ/r is much less than 1, this influence is very small.

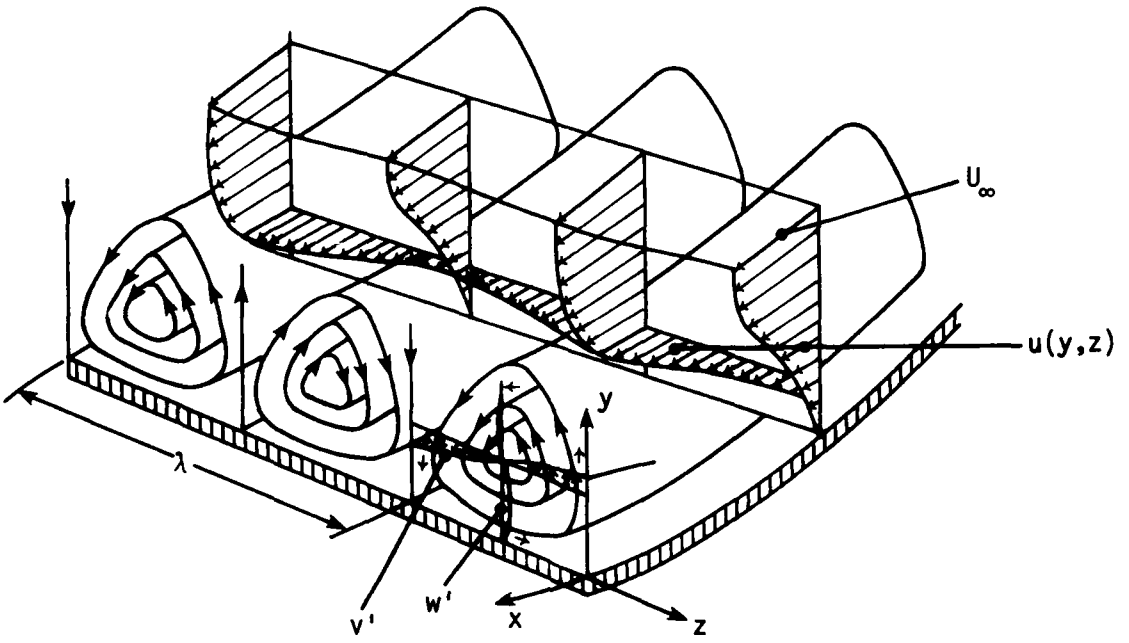

Fig. 14. Flow pattern of Görtler vortices from Wortmann (17).

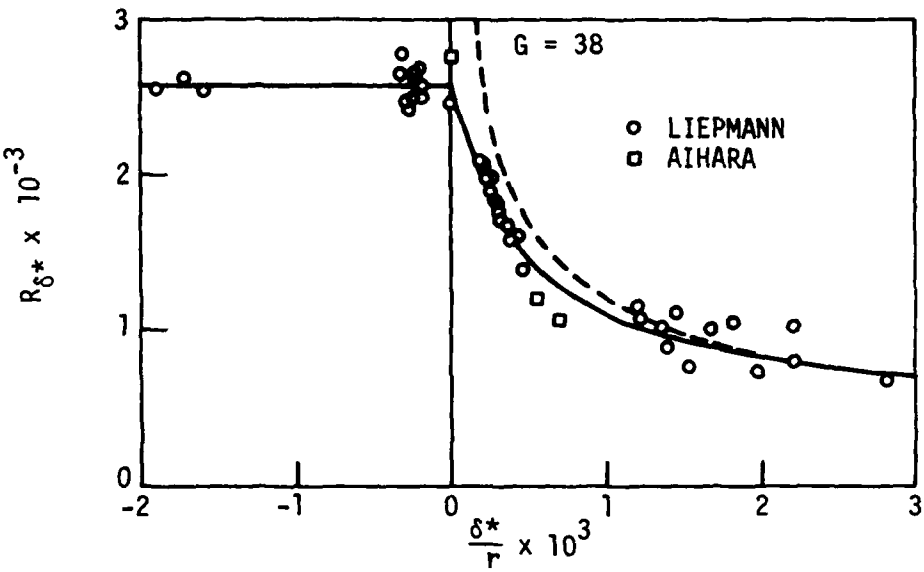

Fig. 15. Effect of surface curvature on transition in a zero pressure gradient from Tani (12).

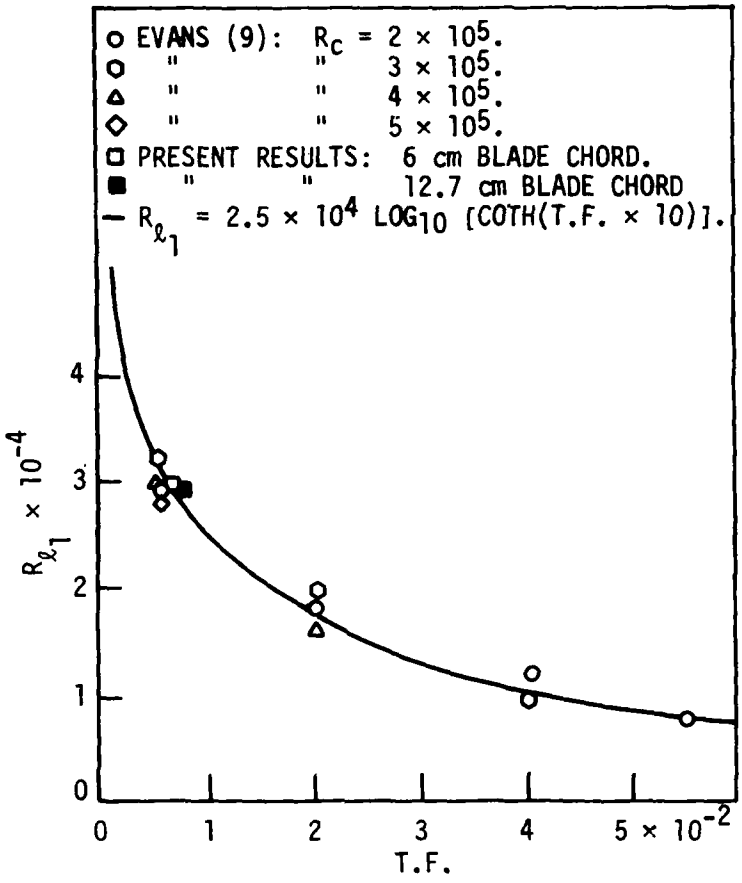

Fig. 16. Variation of the transition length in a laminar separation bubble with turbulence factor from Roberts (20).

4. TRANSITION IN TURBOMACHINE BLADE ROWS

The discussion will now focus on boundary layer flows through axial flow turbomachine blade rows with emphasis on compressor blades, particularly the suction surface. Boundary layers form over the hub and outer walls as well, but these phenomena will not be discussed here. The importance of accurately determining the location of transition will be considered, followed by a discussion of the boundary layer phenomena which occur over the blades and several prediction techniques.

4.1. The Importance of Accurately Locating Transition

Location of transition is important in the study of losses in turbomachinery. According to Koch and Smith (35), loss sources include blade profile losses, end wall boundary layers, shock losses, and drag losses from part span shrouds. Blade profile losses are a boundary layer phenomenon which generates a stagnation pressure, P_o, loss through the blades and creates wakes (vorticity). Both of these effects generate entropy with a resultant loss of thermal efficiency.

Lieblein (36) observes that losses arise from the growth of the boundary layer. Also, P_o losses can be correlated to the boundary layer momentum thickness and shape factor at the trailing edge. Since the boundary layer growth characteristics are quite different for laminar, transitional, and turbulent boundary layers, analytic loss predictions depend on an accurate calculation of the location and extent of each region. Roudebush and Lieblein (11) estimate that the calculation of the drag coefficient may be in error by 10% because of an error in location

of transition by 20% of chord at $Re_c = 10^7$.

4.2. Parametric Effects in Turbomachinery Flows

Typical boundary layer effects observed in axial flow compressors and the resultant effects on transition are summarized below. This summary includes the effects of freestream turbulence, surface roughness, and laminar separation.

4.2.1. Reynolds Number Effects

Schlichting and Das (31) summarize the effect of chord Reynolds number Re_c as follows: for $Re_c < 5 \times 10^5$, transition is significant on the suction surface; for $Re_c < 2 \times 10^5$, laminar separation begins; for $Re_c < 1 \times 10^5$, complete laminar separation is expected to occur. These results are for low turbulence levels Tu < 2% based on cascade tests.

In compressor tests where $Re_c = 1.5 \times 10^5$, Walker (8) observed that the transition region occupied between 15% to 45% of total chord length. The start of transition was independent of Re_c, but the instability region $Re_{\theta t} - Re_{\theta i}$ decreased as Re_c decreased. Turbulence intensities were in the range of 2% to 6%.

Pollard and Gostelow (37) observed laminar separation on cascade tests for $Re_c = 1.1 \times 10^5$ with low turbulence levels and noted that decreasing Re_c caused an increase in bubble length.

Schäffler (32) observed that turbulence intensity had no effect on the length of the separation bubble in cascade tests for $Re_c = 5 \times 10^4$.

4.2.2. The Effect of Freestream Turbulence and Unsteadiness

Turbulence increases in intensity as the flow progresses through

each stage of a compressor. Dunham (6) presents an equation to approximate the increase in turbulence based on the contraction ratio. Turbulence levels at high flight altitudes are generally nil and may cause laminar separation in the first stage of compressors.

Evans (30, 38) measured the turbulence and unsteadiness in single-stage compressors. His measurements indicate a turbulence intensity (including random fluctuation and unsteadiness) of 2.5% to 7%, with decreasing turbulence for increasing flow coefficient. He notes that the velocity drops sharply on the pressure side, but rises more slowly on the suction surface, indicating a thicker boundary layer. He also notes that the tangential fluctuating velocity reaches a maximum in phase with the passing wake. Velocity defect in the wake is approximately 20%. This is similar to the findings of Roudebush and Lieblein. Evans also estimates that the measured velocity profiles fluctuate periodically at transition between a fully laminar and fully turbulent profile. The largest unsteady profile fluctuation occurred at $y/\delta = 0.3$.

Walker indicates that the main effect of periodic unsteadiness caused by the passing of wakes is "smearing out" of the transition region (30).

4.2.3. Surface Roughness

In three-stage compressor tests with NACA 65 blades, Bammert and Woelk (39) observed that surface roughness distributed on the blade surface beyond a 60 grain size caused a decrease in efficiency of 2 to 6%. Schäffler reports a decrease of 3%. Neither author, however, conducted hot-wire measurements; consequently, no velocity profiles were

determined.

4.2.4. Laminar Separation

Laminar separation causes an efficiency loss in compressors. Unfortunately, a theoretical treatment of separation is not presently possible. The following results are based on the NACA 65 cascade tests of Roberts (20) and Kiock (22), and the compressor tests of Walker (8, 23). All tests employ Thwaite's separation criteria.

Roberts defines a "bursting" Reynolds number $Re_{c(B)}$ where the loss coefficient increases rapidly because of a long separation bubble. Typically, the separation point is independent of chord Reynolds number but dependent on angle of attack. Roberts' correlation is based on a turbulence factor (TF) which accounts for the scale of the turbulence. The bursting Reynolds number $Re_{c(B)} = U_o c/\nu$ is determined from the following correlations:

$$Re_{c(B)} = \frac{D + 0.4}{7.5\ (TF)^{\frac{1}{2}}} \times 10^5 + 10{,}000 \qquad (22)$$

where D is the diffusion factor related to upstream and downstream velocities as defined by Roberts (2). Roberts also establishes a correlation to determine the location of transition in the bubble from the separation point (see Figure 16).

Kiock conducted cascade tests using an oscillating grid to simulate unsteadiness, varying the turbulence intensity from 0.3% to 8%. He concluded that at constant Re_c turbulence intensity reduced bubble length. Increasing the chord Reynolds number at constant Tu reduces bubble length. Laminar separation was observed for chord Reynolds number of

$90{,}000 < Re_c < 1.6 \times 10^5$.

Walker uses Horton's (42) criteria to determine the following transition location:

$$\frac{x_t - x_s}{\theta_s} = \frac{4 \times 10^4}{Re_{\theta,s}} \tag{23}$$

where the mean shape factor across the bubble is less than 4.20. He proposes a different equation based strictly on a curve fit if the shape factor is greater than 4.20. The turbulent reattachment point criteria is based on

$$\frac{\theta}{U}\frac{dU}{dx} = -0.0082 \tag{24}$$

Generally, laminar separation occurred on the British C4 section profiles below $Re_c < 2 \times 10^5$. The separation point moves downstream and increases in bubble length as the angle of incidence decreases, supporting Roberts' observation. Walker also recommends using a linear, rather than a parabolic, curve fit to the U(x) data to locate the point of separation.

4.2.5. Turbine Blading

Turbine blade rows present a different transition problem than compressor blades because of pressure gradient and heat transfer effects. Since turbine blades are often cooled internally, heat transfer from the fluid tends to stabilize the flow. Seyb (19) notes that pressure distributions are such that separation does not occur unless induced by shocks. Bayley (40) notes that for $2 \times 10^5 < Re_c < 2 \times 10^6$ the pressure surface stays laminar, while suction surface transition occurs in the

range of 50% to 70% of chord. Bayley asserts that turbulence levels for turbines are higher, usually around 20%.

4.3. Prediction Methods

All of the following methods for predicting transition are based on either direct experimental observations or compressor/cascade data correlations methods using Thwaites' method for calculation of the laminar boundary layer thickness, Martensen's method for calculating laminar velocity profiles, and Truckenbrodt's method for turbulent boundary layers.

4.3.1. General Methods

Experimental techniques exist which give estimates of the transition region, usually based on hot-wire anemometer measurements in cascades and compressors. Transition causes a sharp decrease in the shape factor H, which indicates formation of a turbulent velocity profile. Alternatively, transition can be located by a sharp increase in the skin friction coefficient. If a pitot tube is placed in the boundary layer, an increase in dynamic pressure can indicate the beginning of the transition region. Some investigators use the minimum suction pressure point. However, as previously discussed and as illustrated in Figure 1, this is only valid at high Re_c numbers. A hot-wire anemometer may be used to indicate the appearance of turbulent bursts, and hence determine the intermittency factor. However, these bursts begin to appear in the shear layer of the boundary layer, so the investigator should estimate this layer using the suggestions of Tani (12) and Walker (8).

All of the experimental techniques mentioned above require that the observer understand the transition mechanism in order to adequately analyze the data.

4.3.2. Dunham's Correlation

Dunham's (6) estimations are based on a curve fit of turbine blade cascade and compressor test data from other sources. Parameters are pressure gradient $m_\theta = \theta^2/\nu(dU/dx)$ and an average turbulence intensity between leading edge and trailing edge of the blade. Dunham safely defines transition as the region where the intermittency varies from 0.25 to 0.75.

His correlation equation is

$$Re_{\theta,tr} = (0.27+0.73\ \exp(-.8\bar{Tu}))\ (550+680(1+\bar{Tu}-21m_\theta)) \qquad (25)$$

where $\bar{Tu}$ represents the average turbulence intensity. Good correlation was established with Evan's compressor data, but less success was obtained with turbine data.

The author of this paper recommends using this equation with caution since only one source for compressor data was used and a compressor with a different blade profile may yield different results. Dunham's turbine data are more comprehensive since several sources were used.

Dunham also suggests a correlation for predicting the transition length in a laminar separation bubble, based on Walker's data:

$$R_{l_1} = \frac{U_s l_1}{\nu} = 5000 + \exp(10.463 - 1.54\ Tu^{0.629}) \qquad (26)$$

Unfortunately, Dunham again used only one source. This author assumes

that the compressors used by Walker and Evans were equipped with British C4 section blades; it should be noted that other profiles may have different characteristics. Dunham's definition of transition, though, agrees well with White's (1).

4.3.3. Seyb's Correlation

Seyb (19) takes a similar approach and arrives at a correlation in the form of a chart (see Figure 17). This chart is very similar to Dunham's, but gives no reference to the sources of the data. Also, Seyb's chart does not extend to the higher turbulence levels found in turbomachinery. The equation for this correlation is

$$Re_{\theta,tr} = \frac{1000}{1.2 + 70Tu} + 10\left(\frac{0.09 + m_\theta}{0.0106 + 3.6Tu}\right)^{2.62} \qquad (27)$$

for turbulence intensity less than 4%.

4.3.4. Forest's Method

Forest uses a turbulence model approach and accounts for acceleration forces, curvature, turbulence, and pressure gradient. Forest's principal contribution is the development of a scheme to calculate the boundary layer development in the transition region, the velocity profiles in that region, and the end of transition. He uses Seyb's criterion to predict the beginning of transition.

An effective viscosity is used to account for increasing turbulence in the transition region, utilizing an intermittency factor γ. Boundary layer calculations are based on modified equations of Patanker and Spalding.

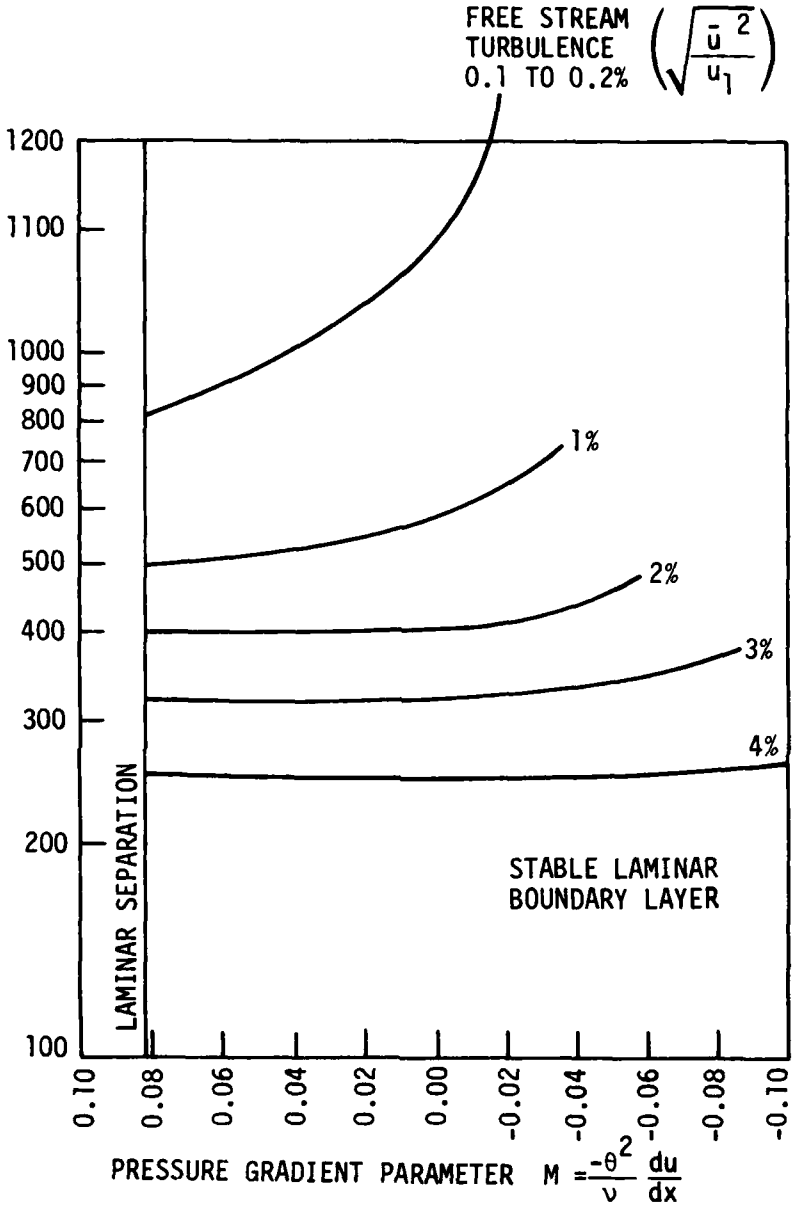

Fig. 17. Transition Reynolds number Re_θ as a function of pressure gradient and turbulence intensity from Seyb (19).

Forest uses a revised pressure gradient parameter $m = m_o \nu/\bar{\nu} = f(Re_\delta, \gamma$, and Tu), which accounts for the eddy viscosity effect.

Forest found fair agreement with turbine data and, like Walker, found large areas of laminar and transitional flow. It is interesting tc note that at a turbulence level of 6%, transition occurred from 30% to 80% over the chord length for turbine blades. Forest's model, however, does not account for heat transfer effects, which Schlichting considers an important component. Forest's contribution is significant, since he accounts for the Görtler number on the concave surface.

4.3.5. Walker's Correlation

Walker (8, 23) presents the most comprehensive evaluation of transition on compressor blades. Walker conducted tests on the British C4 section stator blades of a single stage research compressor. Chord Reynolds number varied from 2.5×10^4 to 1.9×10^5, angle of incidence varied from -11° to +5°, and turbulence intensity ranged from 2% to 6%.

Walker observed that the flow was basically two-dimensional over 80% of the stator span because of an absence of secondary or radial flows. He then used a stethoscopic technique and baked-clay tests to locate transition experimentally. He analytically located the instability point $Re_{\theta,crit}$ as a function of Stuart's pressure gradient parameter $m_\theta = \theta^2/\nu(dU/dx)$. He used a mean value since the instability point fluctuates in unsteady flow. Analytically, transition was defined as the location where turbulent spots appear.

Walker also observed that at highly negative incidence (approx -6°) the instability region occupied 45% of the chord length. At positive

angles of incidence (approx +4°), the instability region was reduced to 20% of chord.

Walker detected Tollmien-Schlichting waves in the trough of the instantaneous unsteady velocity trace, and observed that the breakdown process occurred during the acceleration phase. At the unsteady Reynolds number of Re_{NS} = 1000, he observed that transition occurred in the "aperiodic" mode as suggested by Obremski and Fejer (28). He observed that the location of transition increased as the angle of incidence decreased, but that transition location was independent of Re_c. He also noted that, in general, $(Re_{\theta,t} - Re_{\theta,i})$ decreased as Re_c decreased.

Walker then correlated the location of transition, based on the location of instability, to the mean shape factor H_m across the instability region. Using a least square fit to Granville's isolated airfoil data and his own, Walker obtained the following transition Reynolds number correlation:

$$(Re_{\theta,tr} - Re_{\theta,i})/Re_{\theta,mean} = 1.70 - 0.32 \times H_m \qquad (28)$$

This correlation applies to $3 \times 10^4 < Re_c < 5 \times 10^7$. Walker also proposed a transition location based on the mean shape factor. In all cases, the mean shape factor is a function of pressure gradient dp/dx and Re_c which are the dominant factors affecting amplification rates.

Walker's correlation does not include freestream turbulence, for reasons discussed in the previous section on freestream turbulence effects. Stated briefly, he feels that turbulence indirectly affects transition through a direct modification of the incidence angle and pressure gradient. The turbulence levels in his compressor tests,

however, were not varied independently of Reynolds number. The turbulence intensity decreased with decreasing Reynolds number. This may represent a flaw in Walker's correlation.

Finally, Walker observed that the transition length $x_T - x_t$ is nearly constant, occurring about 10% to 20% of chord for negative angles of incidence. Walker's model also predicts an overly large x_t since the shape factor H is too large in his calculation scheme (Thwaites' method). Consequently, laminar separation is predicted too often in Walker's model.

4.3.6. The Albers and Gregg Method

Albers and Gregg (41) modified an existing finite difference boundary layer calculation computer program to provide an improved transition prediction method. The instability point is determined from $Re_{\theta,crit} = f(m_\theta, S_t)$. For transitional boundary layer computation, a turbulence model is employed including the calculation of an effective viscosity and intermittency factor. Transition is defined as the location where $\gamma = 0.01$.

To determine the location of transition, Re_θ and $Re_{\theta,tr}$ are calculated at each streamwise station. Calculation of $Re_{\theta,crit}$ includes the effects of pressure gradient, freestream turbulence, surface roughness, suction, and surface curvature. Each effect is normalized into a reduction factor, based on the transition Reynolds numbers for each effect presented in graphic form by Schlichting (5, 1960 edition). The corrected transition Reynolds number is computed from the following equation

$$Re_{\theta,tr} = Re_o \times R_k \times R_{m\theta} \times R_H \times R_{Tu} \times R_{curv}$$

where Re_o represents the flat plate transition Reynolds number and $R_{( )}$ represents the appropriate reduction factors. This calculation is done at each station.

4.3.7. The McDonald and Fish Method

McDonald and Fish present a finite difference computation scheme for calculating transitional boundary layer characteristics. Transition is located at the point of minimum skin friction coefficient.

McDonald and Fish employ a turbulence model approach using a turbulent energy equation consisting of a convection integral, a net production integral, and a normal-stress production integral. In the initial stage of transition, the normal-stress production term equals zero. The velocity distribution and boundary layer thicknesses are then computed at each station. McDonald and Fish note that in the transition region, the viscous stresses and apparent turbulent stresses are approximately equal.

Freestream turbulence is accounted for as a source term in the turbulent energy equation. This changes the magnitude of the Reynolds stress, thus decreasing the transition region length. If the roughness is increased sufficiently, a roughness-induced transition begins.

5. SUMMARY

The foregoing review should indicate the complexity of transition prediction, even in two-dimensional, incompressible flows. The interactions of the parameters are not fully understood or universally agreed upon; the interaction of freestream turbulence and pressure gradient is only one example of this disagreement. Consequently, data correlations of airfoil, cascade, and compressor boundary layer measurements offer the best solution to transition prediction. Finite difference computations provide a means for calculating transitional boundary layer growth, but still rely on the data correlations to pinpoint the initiation of transition.

Stability theory provides a useful guide for determining the overall effects of various parameters, even though it accounts for only one step in the entire transition process. Parametric effects other than pressure gradient have not been successfully modeled.

The mechanism of flat plate, zero pressure gradient transition appears to be universally accepted thanks to the large number of flow visualization tests conducted. However, some disagreement exists regarding the parametric influences, and the mechanism of turbulence is not agreed upon because of the complexity of describing its characteristics.

Airfoils and compressor blades, therefore, present a difficult problem since all of the parameters mentioned in this paper act simultaneously. Data correlations from different sources usually show variations on the order of 10 to 30% in the transitional Reynolds number because of variety in blade section shapes and free stream disturbance spectra, blade roughness, and hidden (or unreported) three-dimensional

effects. This author suggests that the second derivative of the pressure gradient d^2p/dx^2 may help account for the blade section shape. Walker (8), however, considers the shape factor H capable of accounting for this effect.

In the absence of a fully developed transition theory (a development Morkovin (2) considers improbable), this author recommends the use of Walker's data correlation. Walker has presented the most detailed study of the transition process on compressor blades and has also supported many of his findings with accepted boundary layer theories, particularly those of Schlichting (5) and Obremski and Fejer (28). However, some doubt about broad application of Walker's findings remains since he did not vary turbulence intensity independently of the chord Reynolds number. However, his observations of freestream disturbances effects are well taken, and his observations regarding laminar separation are in agreement with the observations of Roberts (20) and Kiock (22).

Finally, work on transition is essentially incomplete and, as White (1) remarks, "the final report on transition may never be handed in." The problem remains unresolved. Consequently, the transition prediction methods summarized in this paper should be applied cautiously and with an awareness of the fluid mechanics involved in each particular flow problem.

6. BIBLIOGRAPHY

1. White, Frank M. Viscous Fluid Flow. New York. McGraw-Hill, 1974.

2. Morkovin, M. V. "Instability Transition to Turbulence and Predictability." NATO AGARDograph No. 236, 1978.

3. McDonald, H., and R. W. Fish. "Practical Calculations of Transitional Boundary Layers." NATO AGARDograph No. 164, 1972, pp. 33-45.

4. Hall, D. J., and J. C. Gibbings. "Influence of Stream Turbulence and Pressure Gradient upon Boundary Layer Transition." Journal of Mechanical Engineering Science 1972, pp. 134-146.

5. Schlichting, H. Boundary Layer Theory, 7th edition. New York. McGraw-Hill, 1979.

6. Dunham, J. "Prediction of Boundary Layer Transition on Turbomachinery Blades." NATO AGARDograph No. 164, 1972, pp. 33-45.

7. Obremski, H. J., M. V. Morkovin, and M. Landahl. "A Portfolio of Stability Characteristics of Incompressible, Laminar Boundary Layers." NATO AGARDograph No. 134, 1969, pp. 1-14.

8. Walker, G. L. "Boundary Layer Behavior on Blading of a Single Stage Axial Flow Compressor." Ph.D. thesis, University of Tasmania, 1971.

9. Mack, L. M. "Transition Prediction and Linear Stability Theory." NATO AGARD Conference Proceedings No. 224, 1977, pp. 1-1 to 1-22.

10. Reshotko, Eli. "Boundary Layer Stability and Transition," in Milton Van Dyke and Walter G. Vincenti, eds., Annual Review of Fluid Mechanics, v. 8. Palo Alto. Annual Reviews, Inc., 1976, pp. 311-349.

11. Roudebush, W. H., and Seymour Lieblein. "Viscous Flow in Two-Dimensional Cascades." Chapter V in Aerodynamic Design of Axial-Flow Compressors. NASA-SP 36, 1965.

12. Tani, I. "Boundary Layer Transition," in William R. Sears, ed., Annual Review of Fluid Mechanics, v. 1. Palo Alto. Annual Reviews, Inc., 1969, pp. 169-195.

13. Knapp, C. F., and P. J. Roache. "A Combined Visual and Hot-Wire Anemometer Investigation of Boundary Layer Transition." AIAA Journal, January 1968, pp. 29-36.

14. Van Driest, E. R., and C. B. Blumer. "Boundary Layer Transition: Freestream Turbulence and Pressure Gradient Effects." AIAA Journal, June 1963, pp. 1303-1306.

15. Forest, A. E. "Engineering Predictions of Transitional Boundary Layers." Turbulent Laminar Transition. NATO AGARD Conference Proceedings No. 224, 1977, pp. 22-1 to 22-19.

16. Mack, Leslie M. "Boundary-Layer Stability Theory." Pasadena. Jet Propulsion Laboratory, November 1969.

17. Wortmann, F. X. "Visualization of Transition." Journal of Fluid Mechanics, 1969, pp. 473-480.

18. Dryden, H. L. "Transition from Laminar to Turbulent Flow." in C. C. Lin, ed., Turbulent Flows and Heat Transfer vol. V of High Speed Aerodynamics and Jet Propulsion. Princeton. Princeton University Press, 1959, pp. 3-70.

19. Seyb, R. "The Role of Boundary Layers in Axial Flow Turbomachines and the Prediction of their Effects." NATO AGARDograph No. 164, 1972, pp. 241-259.

20. Roberts, W. B. "The Effect of Reynolds Number and Laminar Separation on Axial Cascade Performance." Journal of Engineering for Power, April, 1975, pp. 261-274.

21. Citavy, J., and J. F. Norbury. "The Effect of Reynolds Number and Turbulence Intensity on the Performance of a Compressor Cascade with Prescribed Velocity Distribution." Journal of Mechanical Engineering Science, 1977, pp. 93-100.

22. Kiock, R. "Influence of the Degree of Turbulence on the Aerodynamic Coefficients of Cascades." Boundary Layer Effects in Turbomachines. NATO AGARDograph No. 164, 1972, pp. 73-85.

23. Walker, G. J. "A Family of Surface Velocity Distributions for Axial Compressor Blading and their Theoretical Performance." Journal of Engineering for Power, April, 1976, pp. 229-241.

24. Gault, D. E. "Experimental Investigation of Regions of Separated Laminar Flow." NACA TN 3505, 1955.

25. Crabtree, L. F. "Predictions of Transition in the Boundary Layer of an Airfoil." Journal of the Royal Aeronautical Society, July, 1958, pp. 525-528.

26. Van Ingen, J. L. "Transition, Pressure Gradient, Suction, Separation, and Stability Theory." NATO AGARD Conference Proceedings No. 224, 1977.

27. Hansen, Elmer C. "A Study of Methods for Analysis of the Flow Fields in Cascades." Iowa State University. Report ISU-ERI-AMES-77065, TCRL-6, September, 1976.

28. Obremski, H. J., and A. A. Fejer. "Transition in Oscillating Boundary Layer Flows." Journal of Fluid Mechanics, 1967, pp. 93-111.

29. Dzung, L. S., and C. Seippel. "Aerodynamic Aspects of Blading Research," in L. S. Dzung, ed., Flow Research on Blading, Amsterdam. Elsevier Publishing Company, 1970, pp. 1-42.

30. Evans, R. L. "Turbulence and Unsteadiness Measurements Downstream of a Moving Blade Row." Journal of Engineering for Power, January, 1975, pp. 131-139.

31. Schlichting, H., and A. Das. "On the Influence of Turbulence Level on Aerodynamic Losses of Axial Turbomachines," in L. S. Dzung, ed., Flow Research on Blading, Amsterdam. Elsevier Publishing Company, 1970, pp. 243-271.

32. Schäffler, A. "Experimental and Analytical Investigation of Reynolds Number and Blade Surface Roughness on Multi-Stage Axial Flow Compressors." Journal of Engineering for Power, January, 1980, pp. 5-12.

33. Rogler, H. L. "The Coupling Between Freestream Disturbances, Driver Oscillations, Forced Oscillations, and Stability Waves in a Spatial Analysis of a Boundary Layer." NATO AGARD Conference Proceedings No. 224, 1977.

34. Horlock, J. H., and R. L. Evans. "The Momentum Integral Equation for a Boundary Layer with Turbulence or Ordered Unsteadiness in the Free-Stream." Journal of Fluids Engineering, March, 1975, pp. 126-129.

35. Koch, C. C., and L. H. Smith, Jr. "Loss Sources and Magnitudes in Axial-Flow Compressors." Journal of Engineering for Power, July, 1976, pp. 411-424.

36. Lieblein, S., and W. H. Roudebush. "Theoretical Loss Relations for Low-Speed Two-Dimensional-Cascade Flow." NACA TN 3662, 1956.

37. Pollard, D., and J. P. Gostelow. "Some Experiments at Low Speed on Compressor Cascades." Journal of Engineering for Power, July 1967, pp. 427-436.

38. Evans, R. L. "Boundary Layer Development on an Axial-Flow Compressor Stator Blade." Journal of Engineering for Power, April, 1978, pp. 287-293.

39. Bammert, K., and G. V. Woelk. "The Influence of Blading Surface. Roughness on the Aerodynamic Behavior and Characteristic of an Axial Compressor." Journal of Engineering for Power, April, 1980, pp. 283-287.

40. Bayley, F. J., and W. J. Priddy. "Effects of Free Stream Turbulence and Frequency on Heat Transfer to Turbine Blading." Journal of Engineering for Power, January, 1981, pp. 60-64.

41. Albers, J. A., and J. L. Gregg. "Computer Program for Calculating Laminar, Transitional, and Turbulent Boundary Layers for Compressible Axisymmetric Flow." NASA TN D-7521, April, 1974.

42. Horton, H. P. "A Semi-Empirical Theory for the Growth and Bursting of Laminar Separation Bubbles." Aeronautical Research Council CP-1073, 1969.

43. Kline, S. J. "Turbulent Boundary Layer Prediction and Structure - The State of the Art," in L. S. Dzung, ed., Flow Research on Blading, Amsterdam. Elsevier Publishing Company, 1970, pp. 372-396.

7. ACKNOWLEDGMENTS

I wish to thank Dr. George Serovy for his direction and assistance in the development and successful completion of this paper. Dr. Serovy also provided valuable advice during my masters degree program as major professor of my graduate committee. I also thank Dr. Bruce Munson, Dr. Theodore Okiishi, and Dr. Donald Young for their assistance both as members of my graduate committee and as instructors.

I especially wish to thank my wife Barbara for her constant and enduring support throughout my masters degree program.

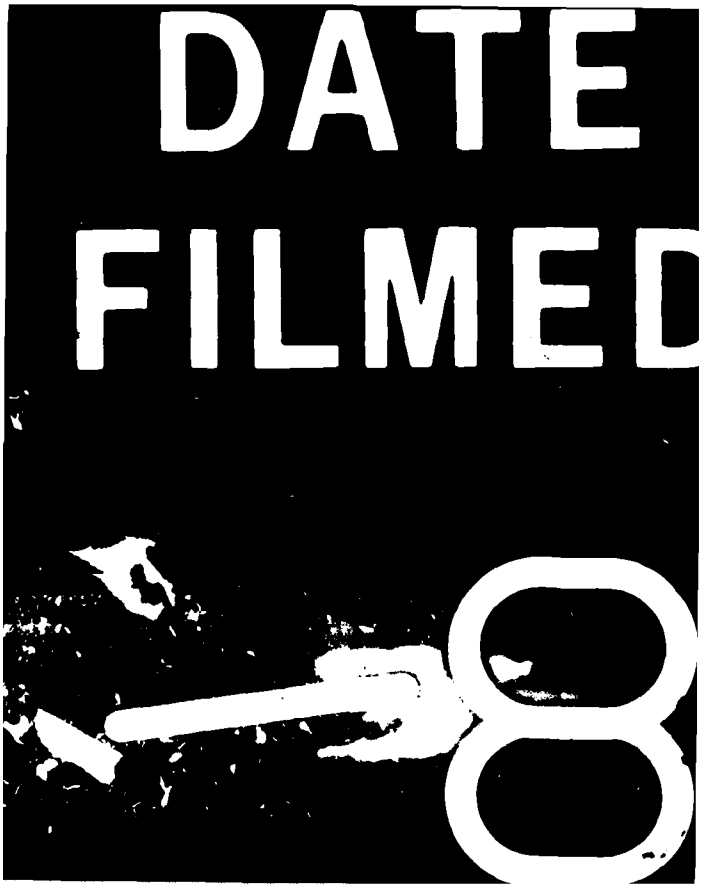
DATE
FILMED
8